SYNTHESIS AND CHARACTERIZATIONS OF COPPER-BASED NANOSTRUCTURES DEVELOPED BY MECHANICAL MILLING

A

Thesis Submitted in Partial Fulfillment of the Requirement for the Award of Degree of

Master of Technology
in
Metallurgical and Materials Engineering

By

Pankajini Sahani

Roll No: 208MM106

Department of Metallurgical and Materials Engineering
National Institute of Technology Rourkela-769008
May 2010

SYNTHESIS AND CHARACTERIZATIONS OF COPPER-BASED NANOSTRUCTURES DEVELOPED BY MECHANICAL MILLING

A

Thesis Submitted in Partial Fulfillment of the Requirement for the Award of Degree of

Master of Technology
in
Metallurgical and Materials Engineering

By

Pankajini Sahani

Roll No: 208MM106

Under the supervision of

Dr. Suhrit Mula
&
Dr. S. K. Pratihar

Department of Metallurgical and Materials Engineering
National Institute of Technology Rourkela-769008
May 2010

NATIONAL INSTITUTE OF TECHNOLOGY
ROURKELA - 769 008, ORISSA

PABX : 0661 - 2465999
Fax : 0661 - 2472926, 2462999
Website : www.nitrkl.ac.in

CERTIFICATE

This is to certify that the thesis entitled "**Synthesis and characterizations of copper-based nanostructures developed by mechanical milling**" submitted by **Pankajini Sahani (208MM106)** in partial fulfillment of the requirements for the award of **Master of Technology** in **Metallurgical and Materials Engineering** at National Institute of Technology, Rourkela is an authentic work carried out by her under my supervision and guidance.

To the best of our knowledge, the matter embodied in this thesis has not been submitted to any other university/institute for award of any Degree or Diploma. This work, in our opinion, has reached the standard of fulfilling the requirements for the award of the degree of **Master of Technology** in accordance with the regulation of the Institute.

Suhrit Mula 26-05-2010

Dr. Suhrit Mula
Assistant Professor
Department of Metallurgical and Materials Engineering
National Institute of Technology
Rourkela

Dr. S. K. Pratihar
Associate Professor
Department of Ceramic Engineering
National Institute of Technology Rourkela

Acknowledgements

I would like to express my deep gratitude to all who contributed in successful conclusion of this work and submission of this dissertation.

I take this opportunity to express my deep sense of respect and gratitude to my thesis supervisors Dr. Suhrit Mula and Dr. S. K. Pratihar who have suggested the problem for my dissertation and initiated me in the field of nanocomposites. I am indebted to them for their constant suggestions, encouragement, valuable guidance and cooperation without which this presentation would not have reached the present shape. The experience of working with them, I strongly believe, will have far-reaching influence in my future life.

I express my immense gratitude and indebtedness to Professor B. B. Verma, Head of Metallurgical and Materials Engineering Department, Dr. A. Basu, Prof. B. C. Ray, Dr. M. Kumar, Dr. D. Chaira and Dr. S. K. Sahoo of Metallurgical and Materials Engineering Department, and Dr. J. Bera, Department of Ceramic Engineering, Dr. D. Behera and Dr. P. Kumar of Physics Department, National Institute of Technology Rourkela for their continuous help and valuable suggestions throughout my M. Tech. program.

I would like to acknowledge with pleasure the encouragements received from various faculty members in this Department like Prof. S.C. Mishra and Prof. U. K. Mohanty.

My sincere thanks are due to Prof. S. K. Pabi, Metallurgical and Materials Engineering Department, IIT Kharagpur for his kind help in preparing SiC nanoparticles.

The technical support by Mr. U.K. Sahu, Mr. Shyamu Hembram, Mr. Rajesh Pattnaik, Mr. Vanja Naik, Kishore Tanty and Mr. S. Samal, is thankfully acknowledged.

I would like to extend my sincere thanks to all my friends, who offered help patiently throughout the project.

Finally, I would like to share this moment of happiness with my parents and brother. The help of my family through all that has happened during my M. Tech. was astounding.

NIT Rourkela
Date: 25.05.2010

Pankajini Sahani
(Pankajini Sahani)

Abstract

The present work investigates on Cu-based nanocomposites developed by mechanical milling. $Cu_{99}Cr_1$, $Cu_{94}Cr_6$, $Cu_{99}Cr_1$–4 wt.% SiC and $Cu_{94}Cr_6$–4 wt.% SiC compositions were subjected to high energy ball milling for 50 h. The phase evolution and morphological changes of the milled samples were carried out using X-ray diffraction (XRD), scanning electron microscopy (SEM), Fourier transform infrared radiation (FTIR) and nano zeta sizer (NZS) analysis. XRD analysis for crystallite size, lattice microstrain% and lattice parameter of the Cu-based alloys revealed that very little amount Cu-based solid solution was possibly formed. XRD, FTIR and NZS analysis revealed that crystallite size/particle size of the 50 h milled samples was in the nanometer range.

An attempt was made to consolidate the mechanically alloyed powder to produce bulk Cu-based nanocomposites having densities near to the theoretical density. Consolidation was carried out by microwave sintering (800°C and 900°C, 30 min), vacuum sintering (900°C and 1000°C, 60 min) and conventional pressure-less sintering (900°C and 1000°C, 60 min) methods. The microwave sintering compacts achieved a relative density (with respect to theoretical density) of 90.8–95% (900°C, 30 min), compared to 84.2–89% in the vacuum sintered (1000°C, 60 min) and 82.3–87% in the pressure-less sintered (1000°C, 60 min) compacts. The particle size (< 200 nm) obtained through AFM and crystallite size (65–125 nm) calculated from XRD data of the sintered specimens established that the bulk consolidated materials were fine grained composites.

The microwave sintered compacts showed greatly superior mechanical properties (e.g. Vickers hardness of 190–240 Hv) compared to the vacuum sintered (173–218 Hv) and pressure-less sintered compacts (170–216 Hv), due to the presence of nano-features and better densification. Wear resistance of the microwave sintered specimens was found to be increased with addition of Cr and nanosize SiC particles. Electrical conductivity of the microwave sintered specimens showed 60–70% conductivity of IACS compared to 40–50% for conventional and vacuum sintered compacts. Therefore the material developed in the present investigation could be successfully used for thermo-electric applications.

Keywords: Nanocomposite; Microwave sintering; Vacuum sintering; Vickers hardness; Wear resistance; Electrical conductivity; X-ray diffraction; Fourier transform infrared radiation; Nano Zeta Sizer; Atomic force microscopy; Electron microscopy.

Contents

		Page No
Certificate		i
Acknowledgements		ii
Abstract		iii
Contents		iv
List of Figures		vii
List of Tables		ix

Chapter 1 : Introduction

1	Introduction	1
1.1	Aim and Objective	3

Chapter 2 : Literature Review

2.1	Preamble		5
2.2	Synthesis techniques of nanostructured materials		6
	2.2.1	Importance of Mechanical milling	6
	2.2.2	Developments in Mechanical alloying (MA)	7
	2.2.3	Process Variables	7
	2.2.4	Advantages of Mechanical Milling (MM)	11
	2.2.5	Development of nanostructures by MM	11
2.3	Advances in preparation of Cu-Cr based alloys and/or mixtures		12
2.4	Hardness and Wear Resistance		14
2.5	Electrical Conductivity		20
2.6	Consolidation and Sintering		21

Chapter 3 : Experimental

3.1 Development of Cu-based nanocomposites 24

3.1.1 Mechanical Milling 24

3.1.2 Consolidation of Milled Powder 25

3.2 Microstructural Characterization 25

3.2.1 X-ray Diffraction (XRD) 25

3.2.2 Scanning Electron Microscopy (SEM) 26

3.2.3 Atomic Force Microscopy (AFM) 27

3.2.4 Nano Zeta Sizer 27

3.2.5 Fourier Transform Infrared Radiation (FTIR) spectroscopy 28

3.2.6 Dilatometry 29

3.3 Evaluation of Mechanical Properties 29

3.3.1 Vickers Hardness Measurement 29

3.3.2 Evaluation of Wear Resistance 30

3.3.3 Evaluation of Electrical Conductivity 30

Chapter 4: Results and Discussion

4.1 Structural Characterization of Milled Samples 32

4.1.1 SEM analysis 32

4.1.2 XRD analysis 33

4.1.3 FTIR analysis 40

4.1.4 Particle Size Analysis 41

4.2 Consolidation and sintering 42

4.2.1 Dilatation and diffusion 43

4.2.2 Microstructural investigation of the sintered specimens 44

4.3 Mechanical Properties of Sintered specimens 53

4.3.1 Vickers hardness 54

4.3.2 Wear Resistance 56

4.4 Electrical conductivity 58

Chapter 5: Conclusions and Futute Scope of Study

5.1 Conclusions 61

5.2 Future Scope of Study 62

References 63

List of Publications 67

List of Figures

Figure No	Description	Page No
Figure 2.1	Tensile curves obtained for ball milled nano crystalline Cu and course grained Cu at a strain rate of 10^{-3} s^{-1}.	15
Figure 2.2	The average microhardness of sintered in situ and ex situ composites with various milling time.	16
Figure 2.3	Vickers hardness of copper –based composite with increasing SiC content.	17
Figure 2.4	Variation of wear rate with the content of TiB_2 in Cu-TiB_2 composites.	18
Figure 2.5	Effect of milling time on the microhardness of compacts.	19
Figure 3.1	Fritsch Pulverisette-5 planetary ball used for mechanical milling.	25
Figure 3.2	Philips X-pert MPD X-ray diffractometer.	26
Figure 3.3	JEOL JSM-6480LV scanning electron microscope.	27
Figure 3.4	VEECO di Innova atomic force microscope.	27
Figure 3.5	Nano ZS (Malvern), Nano zeta sizer used in the present study.	28
Figure 3.6	Perkin-Elmer Spectrum RXI, Fourier transforms infrared radiation (FTIR) Spectrometer.	28
Figure 3.7	NETZSCH DIL 402C Dilatometer.	29
Figure 3.8	Leco LV 700 Vickers hardness tester.	29
Figure 3.9	Ball-On-Plate Wear Tester TR-208 M1.	30
Figure 4.1	SEM micrographs of $Cu_{99}Cr_1$ powder particles milled for (a) 30 min, (b) 10 h and (c) 50 h, respectively.	32
Figure 4.2	XRD pattern of 16 h milled SiC powder sample.	33
Figure 4.3	XRD pattern of (a) $Cu_{99}Cr_1$, (b) $Cu_{94}Cr_6$, (c) $Cu_{99}Cr_1$–4 wt.% SiC and (d) $Cu_{94}Cr_6$–4 wt.% SiC nanocomposites powder samples during milling.	34-36
Figure 4.4	Variation of crystallite size of different compositions with milling time.	38
Figure 4.5	Variation in lattice microstrain(%)of different compositions with milling time.	39

Figure 4.6	Variation of lattice parameter of Cu-based solid solutions with milling time.	40
Figure 4.7	(a) FTIR plot of $Cu_{99}Cr_1$ milled for different durations along with that of 50 h milled $Cu_{99}Cr_1$–4 wt.% SiC and $Cu_{94}Cr_6$–4 wt.% SiC compositions. (b) %Transmittance vs. crystallite size of Cu-based solid solution of $Cu_{99}Cr_1$ composition with reduction of crystallite size.	41
Figure 4.8	Variation of average particle size with volume % of that for (a) $Cu_{99}Cr_1$, (b) $Cu_{94}Cr_6$, (c) $Cu_{99}Cr_1$–4 wt.% SiC, (d) $Cu_{94}Cr_6$–4 wt.% SiC compositions.	42
Figure 4.9	Dilatation behavior of 50 h milled $Cu_{94}Cr_6$ specimen with increasing temperature up to 950°C.	44
Figure 4.10	SEM micrographs of conventionally sintered ((a), (b)) and microwave sintered samples ((c), (d)) of $Cu_{94}Cr_6$ and $Cu_{94}Cr_6$–4 wt.% SiC sintered at 900°C.	47
Figure 4.11	XRD patterns of specimens conventionally sintered at (a) 900°C and (b) 1000°C.	48
Figure 4.12	XRD patterns of specimens sintered by vacuum sintering technique at (a) 900°C and (b) 1000°C.	49
Figure 4.13	XRD patterns of microwave sintered specimens sintered at (a) 800°C and (b) 900°C.	51
Figure 4.14	AFM micrographs of microwave sintered specimens of (a) $Cu_{94}Cr_6$ and (b) $Cu_{94}Cr_6$–4 wt.% SiC compositions, respectively.	53
Figure 4.15	Wear depth vs. time (s) plot for microwave sintered specimens sintered (a) at 800°C and (b) at 900°C.	57
Figure 4.16	SEM micrographs of microwave sintered specimens of (a) $Cu_{99}Cr_1$, (b) $Cu_{99}Cr_1$–4 wt.% SiC, (c) $Cu_{94}Cr_6$, (d) $Cu_{94}Cr_6$–4 wt.% SiC after wear test.	58

List of Tables

Table No	Description	Page No
Table 4.1	Relative sintered density of $Cu_{99}Cr_{1,}$ $Cu_{94}Cr_{6,}$ $Cu_{99}Cr_{1}$–4 wt.% SiC and $Cu_{94}Cr_{6}$–4 wt.% SiC compositions, conventionally sintered at 900°C and 1000°C, vacuum sintered at 900°C and 1000°C, microwave sintered at 800°C and 900°C.	46
Table 4.2	Variation of crystallite size of Cu-based solid solutions for different compositions after sintering by conventional, vacuum, and microwave sintering methods at different temperatures.	52
Table 4.3	Vickers Hardness (Hv) of different specimens sintered by conventional, vacuum and microwave sintering techniques at different temperatures.	55
Table 4.4	Electrical conductivity of different specimens sintered by conventional, vacuum and microwave sintering techniques at different temperatures.	60

CHAPTER 1 Introduction

1. Introduction

Copper (Cu) or Cu-based alloys are normally used for high electric and thermal conductive applications because of their excellent electrical and thermal conductivity, resistance to corrosion and ease of fabrication (Jovanovic et al., 2009). These materials with conventional grain size are soft materials with relatively low yield strength and very low wear resistance. Conventional Cu-based composites can improve strength to some extent but conductivity decreases to an unacceptable range, because amount of reinforcement required is high. The required properties could be increased by a smaller amount of nanosize reinforcement than that of larger content of micron size (Rajkovic et al., 2008; Das et al., 2007) incorporation. The performance of mechanical properties of these materials is expected to be enhanced if the nanosize grain is retained in bulk material with nanosize distribution of second phase particle. This can provide unique characteristics, such as high thermal and electrical conductivities, as well as, high mechanical strength and excellent resistance to high temperature annealing (Shehata et al., 2009). Recently, Shen et al.(Shen et al., 2005) and Guduru et al. (Guduru et al., 2007) showed that tensile strength could be improved to a very high value of ~1 GPa by reducing the Cu grain size to the nanometer range (<100 nm), while ductility remained almost constant or improved.

Presently, Cu-Cr mixtures produced by conventional powder metallurgy route are used for the majority of the switching cases (Huber et al., 1997). The Cr and/or second phase particle play(s) an important role both in strengthening and in restricting grains coarsening of Cu matrix (Morris et al., 1987). Thus, it is expected to improve the existing properties of Cu based nanocomposites. These materials can be used for spot welding electrodes, high-performance switches, rotating source neutron targets, combustion chamber liners, nozzle liners, aerospace propulsion systems and fusion power plants (Marques et al., 2008; Lee et al., 2004). Addition of alloying elements like Cr, Nb etc. in Cu matrix increases the sintered density, mechanical strength, and reinforcement of carbide particles can increase the elevated temperature strength, hardness and wear resistance (Akhtar et al., 2009). Addition of a small amount Cr

and/or fine ceramic particles (Al_2O_3, SiC, TiO_2 or Y_2O_3) can improve the strength while electric and thermal conductivities are not much affected (Jovanovic et al., 2009; Gautam et al., 2008).

The various different techniques are available for preparation of nanostructures or nanocomposite materials. It was reported that during severe plastic deformation, some Cu diffuses in bcc Cr grains giving rise to super saturated solid solution (Sauvage et al., 2008). Cu-43 wt.% Cr nanocomposite was prepared by high pressure torsion using 25 revolution and reported a hardness value of 3.8 GPa of the compact having a particle size of 10-20 nm (Sauvage et al., 2008). Gautama et al. (Gautama et al., 2008) studied on wear and frictional behavior of (Cu-4%Cr)–4% SiC_p in situ cast composites and reported that wear resistance were markedly improved for the composites compared to only cast copper. Age hardening treatment could be utilized to achieve desired combination of strength and conductivity of the Cu-Cr alloys (Ellis et al., 1995). Ellis et al. reported that deformation alternated with a solution plus quenched Cu-Cr alloys might have an advantage over the Cu-Nb and Cu-Ta alloys, because of high temperature solubility of Cr in Cu than Nb and Ta, which allow age hardening to achieve an additional strengthening component. Mechanical milling/alloying (MM/MA) is a popular method to make nanocrystalline materials because of its simplicity and ability to mix the materials uniformly in the intimate atomic level, easily produce tonnage quantity to essentially all classes of materials (Koch et al., 1997). Very few literatures (Marques et al., 2007, Shehata et al., 2009; Guduru et al., 2007; Scattergood et al., 2008; Zuhailawati et al., 2009) available in the investigation of (Cu-Cr)–based nanostructures produced by MA/MM (Suryanarayana et al., 2001). Lahiri et al. (Lahiri et al., 2009a) reported that a fine scale homogeneous distribution of Cr in Cu matrix developed by MM improves the properties like chopping current, wear resistance and enhances its performances. This fine scale distribution of Cr was reported to increase the sintering rate of the powder compacts enhancing mechanical and electrical properties (Lahiri et al., 2009a). Crystallite size of 150 h milled Cu-10 at.% Cr powder obtained through XRD analysis (13 nm) was compared with that of investigated by atomic force microscopy (67 nm) (Lahiri et al., 2009b).

In this present investigation, attempts have been made to synthesize Cu-Cr and (Cu-Cr)–SiC (4 wt.%) nanocomposites by high energy ball milling for 50 h. The structural and morphological changes of the milled samples are to be analyzed by various techniques, namely, XRD, SEM and Fourier transforms infrared radiation (FTIR) spectrometer. Subsequently, the 50 h milled powders were also consolidated using uniaxial pressing followed by cold isostatic pressing (CIP) (to enhance the green density of the pellets) at an applied pressure of 1500 MPa. Sintering was carried out using 3 different techniques, namely, pressure-less conventional method (at 900°C and 1000°C), vacuum sintering (at 900°C and 1000°C), and microwave sintering (at 800°C and 900°C) techniques. Microstructural analysis of the sintered specimens was also carried using XRD, SEM and AFM to compare the properties to that of the milled specimens. Measurement of physical properties like relative density, mechanical properties like Vickers hardness and wear resistance, and electrical properties like conductivity of all the sintered samples were investigated and compared with their conventional counter parts.

1.1. Aim and Objective

With the above discussed background, the objectives of the present work are envisaged as:

- Development of $Cu_{99}Cr_1$ and $Cu_{94}Cr_6$ (in at.%) nanostructured materials and then these are reinforced with nanosize SiC (~30 nm) particulate by mechanical milling. Nanosize SiC (~30 nm) are prepared by mechanical milling in WC grinding media.
- Characterization of the ball-milled powder by XRD, SEM, FTIR and Nano Zeta Sizer analysis.
- Determination of diffusional behavior and sinterability of the ball milled powder by dilatation measurement before consolidation and sintering.
- Consolidation and stabilization of the prepared nanopowder by suitable techniques, namely, vacuum sintering and microwave sintering using the information of thermal stability to retain nanofeatures.
- Characterization of microstructural features of the sintered compacts by XRD, SEM and AFM.

- Measurement of physical properties like density of the sintered specimens by Archimedes principle.
- Evaluation of mechanical properties and analysis of the sintered compacts: This would be done by evaluating mechanical properties, namely, Vickers hardness and wear resistance.
- Evaluation of electrical conductivity of the sintered pellets.
- Analysis of the results and establishment of suitable composition for the best combination of mechanical and electrical properties for practical applications.

CHAPTER 2 Literature Review

2.1 Preamble

Copper (Cu) is most useful metal as it is second only to silver in its ability to conduct electricity. Though it is malleable and extremely ductile, Cu and Cu-based composites with conventional grain size are soft materials with relatively low yield strength and very low wear resistance. Cu or Cu-based alloys are normally used for high electric and thermal conductive applications because of their excellent electrical and thermal conductivity, resistance to corrosion and ease of fabrication (Jovanovic et al., 2009). For this important applications include cookware, refrigerators, radiators, lead frames, connectors etc. There are various applications, namely, high performance switches, rotating source neutron targets, combustion chamber liners, spot welding electrodes and nozzle liners (Marques et al., 2008), which require the unique combinations of high strength, good electrical and thermal conductivities. Cu and Cu-based alloys with conventional grain size are soft materials with relatively low yield strength and very low wear resistance. Conventional Cu based composites can improve the required strength but conductivity decreases to an unacceptable range. The properties of Cu based composites might be increased by nanosize reinforcement than micro size (Rajkovic et al., 2008; Das et al., 2007). The performance of these materials is expected to be enhanced if the nanosize grain is retained in bulk material with nanosize distribution of second phase particle. This can provide unique characteristics, such as high thermal and electrical conductivities, as well as, high mechanical strength and excellent resistance to high temperature annealing (Shehata et al., 2009). The main requirement for structure of these materials is a homogenous distribution of nanosize second phase particles on nanograin copper matrix (Jena et al., 2004) and its stabilization. The second phase particle could be metallic solute elements as well as nanoscale ceramic particles for grain size stabilization and mechanical strengthening of the matrix. Addition of a small amount Cr and/or fine ceramic particles (alumina, silicon carbide, titania or yittria) can improve the strength while electric and thermal conductivities are not much affected (Gautam et al., 2008). Presently, for medium-voltage interrupters, Cu-Cr mixtures produced by conventional powder metallurgy route are used as the superior materials compared to other known

materials for the majority of the switching cases. The capability of a contact material depends strongly on the geometry, mixture ratio, the material characteristics and method of production (Huber et al., 1997).

2.2 Synthesis techniques of nanostructured materials

A wide variety of techniques are being used to synthesize nanostructured materials including (1) rapid solidification, (2) electrodeposition, (3) sputtering, (4) inert gas condensation, (5) crystallization of amorphous phases, and (6) chemical processing. (7) Mechanical attrition by ball milling, which induces heavy cyclic deformation in powders, is a technique which has also been used widely for preparation of nanostructured materials.

2.2.1 Importance of Mechanical milling

Mechanical alloying (MA) is a solid-state powder processing technique involving repeated cold welding, fracturing, and rewelding of powder particles in a high-energy ball mill. Earlier, the method of MA was developed in the 1970's for the production of thoria dispersed nickel (TD Nickel) based superalloys. MA has now the capability of synthesizing a variety of metastable phases starting from elemental powder blends to pre-alloyed powders with ductile-ductile or ductile-brittle or brittle-brittle combinations of materials.

Unlike many of the above methods, mechanical attrition produces its nanostructures not by cluster assembly but by the structural decomposition of coarser-grained structures as the result of severe plastic deformation. This has become a popular method to make nanocrystalline materials because of its simplicity, the relatively inexpensive equipment (on the laboratory scale) needed, and the applicability to essentially all classes of materials. The major advantage often quoted is the possibility for easily scaling up to tonnage quantities of material for various applications. Similarly, the serious problems that are usually cited are, (i) contamination from milling media and/or atmosphere (Koch et al., 1997); careful attention can

reduce/eliminate this problem, and (ii) the need (for structural applications) to consolidate the powder.

2.2.2 Developments in Mechanical alloying (MA)

Mechanical alloying (MA) (Benjamin et al., 1970) is one of the most promising techniques used to produce heat-resistant dispersion strengthened copper alloys, where homogenous distribution of nanosize second phase particles on nanograin matrix could be achieved successfully. This technique can also be successfully used to produce in situ Cu-matrix composites reinforced with particles of materials such as borides, carbides, oxides and intermetallic compounds (Anderson et al., 2001; Dong et al., 2002; Dehm et al., 1998). The repeated deformation, welding and fracturing that occur in MA lead to an intimate mixing of the components in the atomic level. Compared to other methods, synthesis of metal based nanocomposites by MA offers advantages such as more uniform reinforcement particle distribution and finer particle size, leading to stronger and more heat-resistant materials. The solid solubility limit of alloying elements in matrix can be enhanced by MA (e.g. Cr in Cu matrix). Thus, it is expected to improve the existing properties of Cu based nanocomposites developed by MA followed by consolidation for high strength and electrical applications. The performance of these materials is expected to be enhanced if the nanosize grain is retained in the bulk consolidated components.

2.2.3 Process Variables

Mechanical alloying is a complex process and hence involves optimization of a number of variables to achieve the desired product phase and/or microstructure. Some of the important parameters that have an effect on the final constitution of the powder are:

- Type of mill
- Milling container
- Milling speed
- Milling time
- Type, size, and size distribution of the grinding medium
- Ball-to-powder weight ratio
- Extent of filling the vial

- Milling atmosphere
- Process control agent
- Temperature of milling

All these process variables are not completely independent. For example, the optimum milling time depends on the type of mill, size of the grinding medium, temperature of milling, ball-to-powder ratio, etc.

Type of mill

There are a number of different types of mills for conducting MA. Depending on the requirements, type of product to be produced, quantity of the product and facilities available, the mills are different. Most commonly, however, the SPEX shaker mills are used for alloy screening purposes. The Fritsch Pulverisette planetary ball mills or the attritor mills are used to produce large quantities of the milled powder. Specially designed mills are used for specific applications.

Milling container

Hardened steel, tool steel, hardened chromium steel, tempered steel, stainless steel, WC-Co, WC- lined steel and bearing steel are used for the grinding vessels. There shouldn't be any cross contamination from milling media and vials. On the other hand, if the two materials are the same, then the chemistry may be altered unless proper precautions are taken to compensate for the additional amount of the element incorporated into the powder.

Milling speed

The efficiency of milling increases with increase in speed. But it shouldn't exceed critical speed of the mill. Above a critical speed, the balls will be pinned to the inner walls of the vial and do not fall down to exert any impact force. Therefore, the maximum speed should be just below this critical value. Another limitation to the maximum speed is the temperature rise during milling. This may be advantageous in some cases where diffusion is required to promote homogenization and/or alloying in the powders. But, in some cases, this increase in temperature may be a disadvantage because the increased temperature accelerates the transformation process and results in the

decomposition of supersaturated solid solutions or other metastable phases formed during milling. For this work 400 rpm milling speed is chosen.

Milling time

The time of milling is the most important parameter. Normally the time is so chosen as to achieve a steady state between the fracturing and cold welding of the powder particles. The times required vary depending on the type of mill used, the intensity of milling, the ball-to-powder ratio, and the temperature of milling. The level of contamination increases with milling time and some undesirable phases form. Therefore, it is desirable that the powder is milled just for the required duration and not any longer. Milling time of 50 h was chosen for this work.

Grinding medium

Hardened steel, tool steel, hardened chromium steel, tempered steel, stainless steel, WC-Co, and bearing steel are the most common types of materials used for the grinding medium. It is always desirable to have the grinding vessel and the grinding medium made of the same material as the powder being milled to avoid cross contamination. Stainless steel was used as grinding medium for present study during mechanical milling.

The size of the grinding medium also has an influence on the milling efficiency. It has been reported that a combination of large and small size balls during milling minimizes the amount of cold welding and the amount of powder coated onto the surface of the balls.

Ball-to-powder weight ratio (BPR)

The ratio of the weight of the balls to the powder (BPR), sometimes referred to as charge ratio (CR), is an important variable in the milling process. The minimum BPR ranges from as low as 1:1 to as high as 220:1. In general ratio of 10:1 is most commonly used while milling the powder in a small capacity mill such as a SPEX mill. But, when milling is conducted in a large capacity mill, like an attritor, a higher BPR of up to 50:1 or even 100:1 is used. The ball to powder weight ratio of 10:1 was taken for present study.

Extent of filling the vial

Since alloying among the powder particles occurs due to the impact forces exerted on them, it is necessary that there is enough space for the balls and the powder particles to

move around freely in the milling container. Therefore, the extent of filling the vial with the powder and the balls is important. Thus, care has to be taken not to overfill the vial; generally about 50% of the vial space is left empty.

Milling atmosphere

Different atmospheres have been used during milling for specific purposes. Nitrogen or ammonia atmospheres have been used to produce nitrides. Hydrogen atmosphere was used to produce hydrides. The presence of air in the vial has been shown to produce oxides and nitrides in the powder, especially if the powders are reactive in nature. Thus, care has to be taken to use an inert atmosphere during milling.

Process control agents

A process control agent (PCA) is added to the powder mixture during milling to reduce the effect of cold welding. The nature and quantity of the PCA used and the type of powder milled would determine the final size, shape, and purity of the powder particles. Use of a larger quantity of the PCA normally reduces the particle size by 2-3 orders of magnitude. The amount of the PCA is dependent upon the (a) cold welding characteristics of the powder particles, (b) chemical and thermal stability of the PCA, and (c) amount of the powder and grinding medium used. The most important of the PCAs include stearic acid, hexane, Toluene, methanol, and ethanol. Toluene was used as a process control agent for present investigation.

Temperature of milling

There have been conflicting reports on the formation of an amorphous phase as a function of the temperature of milling. Amorphization during MA involves formation of micro-diffusion couples of the constituent powders followed by a solid-state amorphization reaction. Lower milling temperatures are expected to favor amorphization. However, both increased and decreased kinetics have been reported. Milling was carried out in room temperature for present study.

2.2.4 Advantages of Mechanical Milling (MM)

MM is a simple and an economically feasible process with important technical advantages.

- Usually, we make alloys by melting together the components, whereas, Mechanical alloying involves the synthesis of materials in solid state by high-energy ball milling.
- Bulk material with dimension larger than rapid solidification process (RSP) can be produced by MM.
- Synthesis of novel alloys, e.g., alloying of normally immiscible elements, which is not possible by any other technique like RSP. This is because MM is a completely solid state processing technique and therefore limitations imposed by phase diagrams don't apply here.
- Extended solid solubility was achieved by MM in some alloy system. This technique can be used to induce chemical displacement reactions in powder mixtures at room temperature or at much lower temperature than normally required to synthesize pure metals.
- MM can be used for the refinement of the matrix microstructure down to nanometer range. These nanostructures obtained not by clustered assembly but by the structural decomposition of coarser grained structures as the result of severe plastic deformation.
- Amorphous phase formation is one of the most frequently reported phenomena in mechanically alloyed powder mixtures.

2.2.5 Development of nanostructures by MM

Generally, nanocrystalline materials contain flaws, such as porosity and weak inter-particle bonding (Koch et al., 2003). The mechanical and electrical properties of the copper based nanocomposites can be improved by eliminating artifacts using proper consolidation techniques of the ball-milled product. But, it is a formidable task to obtain fully dense bulk samples containing nanofeatures by MM followed by conventional sintering (Groza et al., 2002). This makes it difficult to properly evaluate the mechanical properties of these materials for engineering applications (Weertman et al., 2002; Morris et al., 1998). Conventional consolidation of the nanocrystalline/amorphous powder can lead to significant grain growth. Synthesis of

copper based nanocrystalline and/or amorphous powder by MM and subsequent consolidation by advanced techniques, namely, high pressure torsion, equi-channel angular pressing (ECAP), spark plasma sintering (SPS) (Weertman et al., 2002; Morris et al., 1998) can be used to get near theoretical dense bulk materials having nanofeatures. But, very few literatures (Guduru et al., 2007; Scattergood et al., 2008; Zuhailawati et al., 2009) are available in the investigation of Cu–based nanocomposites produced by MA and followed by consolidation. In India, although several researchers are working in the field of nanomaterials, these are mostly related to preparation and characterization of nanopowder only.

2.3 Advances in preparation of Cu-Cr based alloys and/or mixtures

Presently, for medium-voltage interrupters, Cu-Cr mixtures produced by conventional powder metallurgy route are used as the superior materials compared to other known materials for the majority of the switching cases (Huber et al., 1997). The performance of these materials is expected to be enhanced if the nano-size grain is retained in the bulk consolidated components.

In situ composite Cu–Cr alloy is a new type of contact cable material that has very high strength and conductivity at room temperature compared with other kinds of contact cables. Peng et al. (Peng et al., 2005) prepared in situ Cu-Cr alloy, which can be used for contact cables in elevated temperature. Fine dispersion of Cr present throughout the Cu grains produces a uniform dispersion of Cr inside the Cu grains, which greatly reduces segregation. It results less embrittling effect of the contact. Metal matrix composites with ceramic reinforcement particles can be used for structural applications in wear industry due to their superior toughness and wear resistance. According to Akhtar et al. (Akhtar et al., 2009) show the addition of alloying elements in Cu increased the sintered density and properties and reinforced with carbide particles can increase the elevated temperature strength, improve the hardness and wear resistance. Gautam et al. (Gautam et al., 2008) worked on Cu-Cr–SiC_p in situ composites as alloying with Cr and reinforced with SiC particles together may got wear and frictional behavior of (Cu-4%Cr)–4% SiC_p. Sauvage et al. (Sauvage et al., 2008) prepared Cu-Cr composite containing 43 wt.% Cr by severe plastic

deformation. The maximum solubility of Cu in bcc Cr is indeed less than 0.2 at. % and the maximum solubility of Cr in fcc Cu is 0.89 at% at 1350K. The inter-phase boundaries play an important role in the grain size reduction mechanism. During SPD, some Cu diffuses in bcc Cr grains which actually gave super saturated solid solution reported by Sauvage et al.. Nanoscale materials are often fabricated by consolidation of nanosize powders (Gleiter et al., 1992). Thermally stable nanocrystalline materials may be obtained by dispersions of nanoscale ceramic particles in a metal matrix. Such nanocomposites are usually fabricated by consolidation of the corresponding nanoscale metal matrix composite powders. Various methods are used for the preparation of nanocomposites powder, e.g. mechanical alloying resulting in breaking and redistribution of ceramic particles in a metal matrix (Froes et al., 1989; Hahn et al., 1997), co-sputtering of metal and ceramic (Shull et al., 1990), selective reduction of mixed oxides and thermal decomposition of salts (Murphy et al., 1992; Kear et al., 1993). In all these approaches, dense aggregates or clusters of nanoscale powders are formed with ceramic nanoparticles incorporated in a metal matrix. This results in additional hardening by dispersed particles, which is disadvantageous when consolidation to full density is considered.

Lahiri et al. (Lahiri et al., 2009) reported that a fine scale homogeneous distribution of Cr in Cu matrix improves the properties like chopping current, wear resistance and enhances its performances. They reported that fine scale distribution may increase the sintering rate of the powder compacts and reducing the operation cost and/or time. Ellis et al. (Ellis et al., 1995) reported that deformation processed Cu-Cr alloys might have an advantage over the Cu-Nb and Cu-Ta alloys because of high temperature solubility of Cr in Cu, might allow use of age hardening to achieve an additional strengthening component. Lee et al. (Lee et al., 2004) studied on creep behavior of Cu-Cr In-situ composite and reported that it is a promising material particularly for elevated temperature applications such as aerospace propulsion systems and fusion power plants. Jovanovic et al. (Jovanovic et al., 2009) studied on Cu-0.4%Cr-0.08%Zr-0.05%Mg alloy where the thermomechanical treatment (TMT) avoids high temperature solution annealing and quenching, without reducing the hardness and electrical conductivity, might be regarded as very interesting. Cr in the supersaturated Cu matrix creates a high degree of thermodynamically meta-stable nano-sized

particles, which provide a high chemical potential for the precipitation reaction and was activated by the process of subsequent aging.

2.4 Hardness and Wear Resistance

There are generally two ways to improve the mechanical properties and wear resistance of copper; either by an age hardening mechanism or by incorporation of hard second phase(s) particles (Morris et al., 1987; Lee et al., 2001; Tjong et al., 2000a; and Tjong et al., 2000b). In age hardening, addition of small amounts of Cr or Zr in Cu can give precipitation of a hard second phase, as its solubility in Cu matrix is poor at lower temperatures. These age-hardenable alloys show lack of strength above 500°C due to the structural instability associated with the coarsening of the precipitate phase (Dong et al., 2001; Correia et al., 1997; Morris et al., 1988). Incorporation of hard phase particles such as carbides, oxides, borides in to Cu, it not only enhance the mechanical performance and wear resistance of copper but also keep its desirable electrical and thermal conductivity. Metal matrix composites with ceramic reinforcement particles are helpful for structural applications in the wear industry, primarily because of their superior toughness and wear resistance. Alumina/silicon carbide particles are often used as dispersoids to reinforce copper, which results in superior elevated temperature strength, increased hardness and improved wear resistance (Upadhyaya et al., 1995; Wan et al., 1998; Broyles et al., 1996; Chang et al., 1996 and Ma et al., 2000). Cu-matrix composites are promising candidates for sliding contact applications, where high electrical/thermal conductivity and good wear resistance are needed (Huber et al., 1997). Guduru et al. (Guduru et al., 2007) studied on mechanical behavior of nanostructured materials. They reported that artifacts free materials with nanosized grains (< 100 nm) have exhibited very high strengths with reasonably good ductility which is shown in Fig. 2.1.

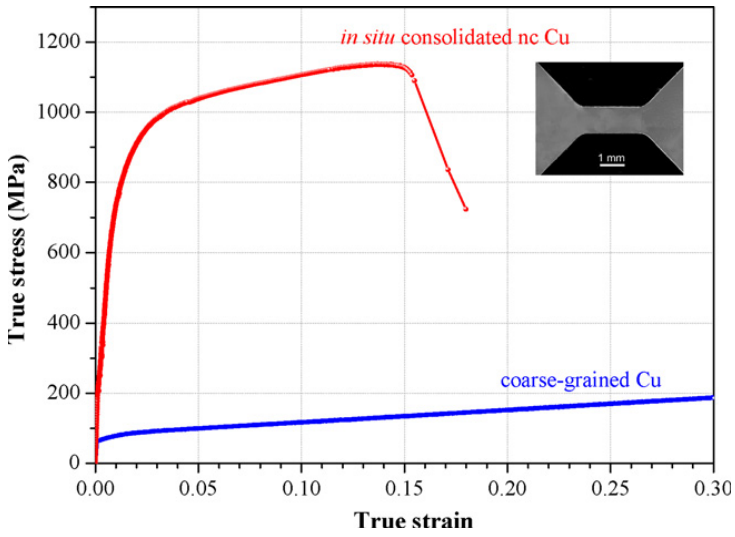

Fig. 2.1: Tensile curves obtained for ball milled nano crystalline Cu and course grained Cu at a strain rate of 10^{-3} s^{-1} (Ref. Guduru et al., 2007).

Zuhailawati et al. (Zuhailawati et al., 2009) studied on the hardness of in situ Cu–15%NbC composite produced by mechanical alloying followed by sintering at 900°C and the properties were compared with that of the ex situ Cu–15%NbC composite. It was found that microhardness of the sintered in situ Cu-NbC pellet is increased slightly after prolonged milling than ex situ pellet as shown in the Fig. 2.2. It was reported that due to formation of NbC in the Cu matrix and also microstructural refinement with crystallite size reduction increases the hardness.

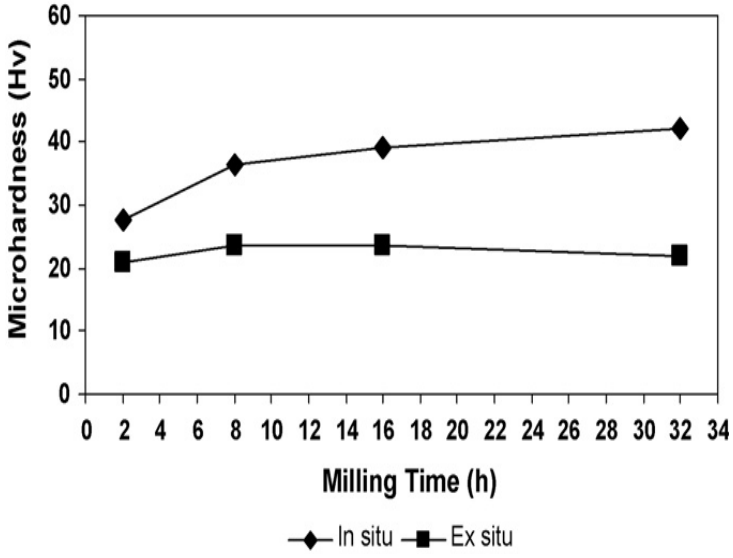

Fig.2.2: The average microhardness of sintered in situ and ex situ composites with various milling time (Ref. Zuhailawati et al., 2009).

The mechanical properties, wear resistance and electrical conductivity of TiC reinforced Cu-matrix composites by powder metallurgy was studied by Akhtar et al. (Akhtar et al., 2009). In Cu–Ti–Al and Cu–Co–Ni as well as in pure Cu matrix 69–77 vol.%. of TiC was incorporated. It was reported that the hardness values (719 HV for Ni & Co containing matrix) of the composites containing alloying elements increase than that of the composite containing pure copper (Goodfellow, 1993/94) as a binder phase. Zhu et al. (Zhu et al., 2007) studied on nano-SiC (~50 nm) reinforced Cu composite processed by electroforming technology. Vickers hardness of composites (Fig. 2.3) increased linearly from 108 to 138 with increasing wt.% of SiC from 0.8 to 2.04 (Zhu et al., 2007).

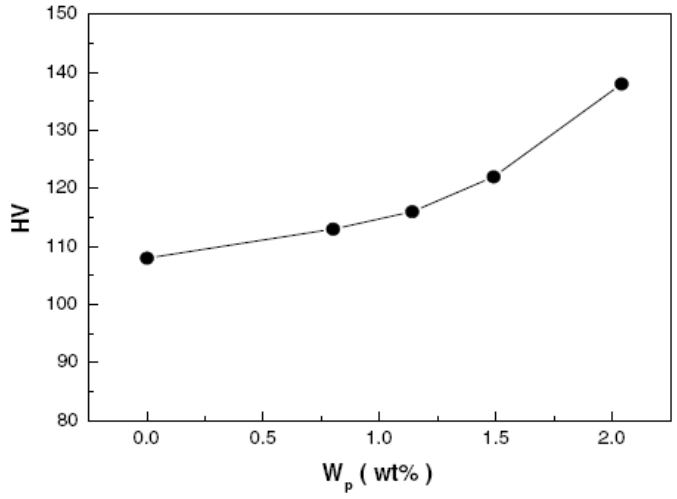

Fig. 2.3: Vickers hardness of copper –based composite with increasing SiC content (Ref. Zhu et al., 2007).

According to Fan et al. (Fan et al., 2005) since nanosized SiC were dispersed in Cu matrix it becomes the obstacle to the dislocation movement when plastic deformation occurs. It was reported that under the same wear condition, the composite exhibited better wear resistance than pure Cu deposit. Mechanical and wear properties of spark plasma sintered Cu-TiB_2 nanocomposites were investigated by Kwon et al. (Kwon et al., 2006). The hardness of Cu-TiB_2 nanocomposites increased, with an increase of the TiB_2 content from 57 HRB for Cu-2.5 wt%TiB_2 to 97 HRB for Cu-10 wt% TiB_2 shown in Fig. 2.4. Within the applied load range, with an increase in the content of TiB_2 nanoparticles the wear resistance of the Cu-TiB_2 nanocomposites was increased.

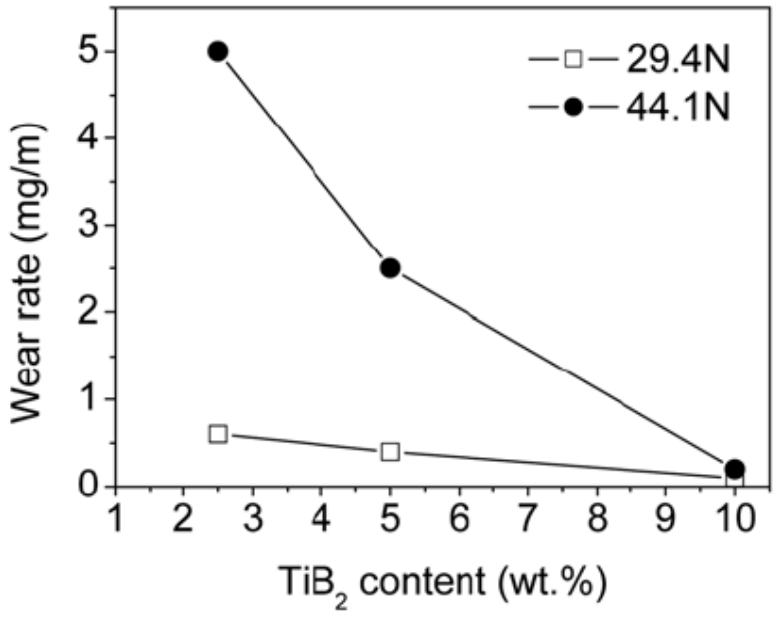

Fig.2.4: Variation of wear rate with the content of TiB_2 in Cu-TiB_2 composites (Ref. Kwon et al., 2006).

Properties of copper reinforced with nano- and micro-sized Al_2O_3 particles were investigated by Rajkovic et al (Rajkovic et al., 2008). Very fine nano-sized Al_2O_3 particles were formed during milling by reaction with internal oxygen. Fig. 2.5 shows the effect of milling time on microhardness of ex situ Cu–5 wt.% Al_2O_3 and in situ Cu–Al_2O_3 composites. After 20 h of milling, microhardness of in situ Cu–Al_2O_3 (2500 MPa) was found to be 1.8 times higher than that of Cu–5 wt.% Al_2O_3 compacts (1430 MPa).

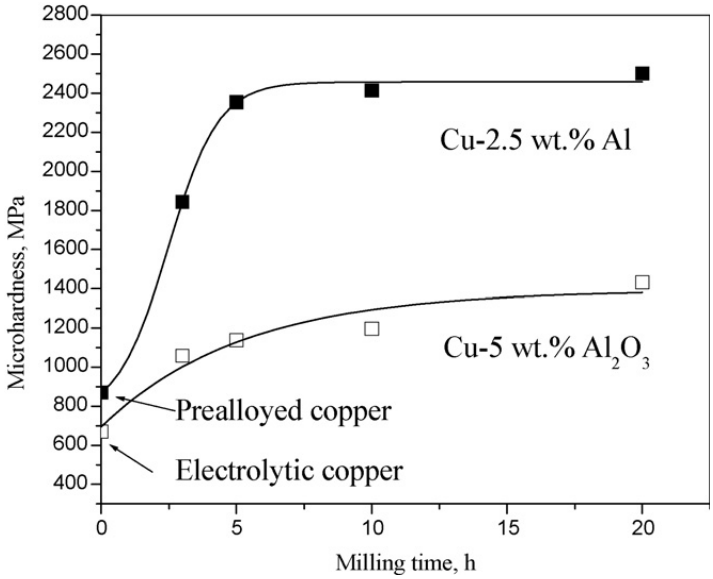

Fig.2.5: Effect of milling time on the microhardness of compacts (Ref. Rajkovic et al., 2008).

Hashemi et al. (Hashemi et al., 2008) studied on wear resistance of Cu–18 vol.% Nb processed by powder metallurgy route. The wear properties of this composite were evaluated against gray cast iron (92 HRB) with the sliding speed and normal load of 1.1 m/s and 4.90 N, respectively. It was found that wear resistance significantly enhanced compared to the copper matrix. Abrasive wear behavior of Cu–5 vol.% of TiB_2 was studied by Tjong et al. (Tjong et al., 2000) using pin-on-disk method with the applied normal loads of 15, 35 and 55 N, the sliding velocity employed was 1 m/s. They has been reported that addition of only 5 vol.% TiB_2 particle to copper gave a dramatic improvement in its wear resistance and this can be further increased by increasing volume fraction of reinforcing particles. Wear resistance of Cu–53 vol.% WC particle reinforced composite and the effect of porosity has been investigated by Deshpande et al. (Deshpande et al., 2006) using pin-on-disk technique with applied normal load on the composite pin changed from 1 to 22N. For fully dense Cu–53 vol.% WC composites, with the normal load of up to around 9N was applied. They reported that wear rate significantly lower than that of pure Cu and the pore containing composites still show a higher wear rate than the fully dense composite.

From the above discussion it is concluded that incorporation of hard second phase particles in the matrix can increase the hardness and wear resistance. But reinforced

with nanosized ceramic particles can improve the properties and also with increase in percentage of second phase it can further enhance the hardness and wear resistance and fully dense composites can show higher hardness and wear resistance than that of composite containing porosity within.

2.5 Electrical Conductivity

Copper (Cu) or Cu-based alloys are normally used for high electric and thermal conductive applications because of their excellent electrical and thermal conductivity. Zuhailawati et al. (Zuhailawati et al., 2009) reported on effect of milling time on electrical conductivity and hardness of Cu-NbC composite. With similar composition and milling time, an ex situ composite also was mixed by ball milling of copper and NbC mixture powder. Electrical conductivity (measured by four point probe method) found in the in situ composite has lower electrical conductivity than ex situ composite due to electron scattering effect caused by the refinement in copper crystallite size by mechanical alloying. Rajkovic et al. (Rajkovic et al., 2008) have also studied on effect of conductivity on Cu matrix with different size and amount of Al_2O_3 particles. Cu (avg. particle size 30 μm) -1 wt.% Al and Cu-3 wt.% Al_2O_3 (avg. particle size0.75 μm) were compacted and sintered at 800ºC. It was reported that for all the composition electrical conductivity increased after sintering with milling time. The electrical conductivity of compacts processed from Cu-3wt.% Al_2O_3 powders reported higher than the conductivity of Cu-1 wt.% Al compacts and also with bigger particle size of Al_2O_3 gave higher conductivity than nano sized as higher electron scatter caused by nano-sized particles. Variation of Electrical conductivity of Cu based composite with 69 vol.% to 77 vol.% of TiC contents was studied by Akhtar et al. (Akhtar et al., 2009). The electrical conductivity was decreased with increasing TiC content because of the volume fraction of nonconducting particles increased. Guler et al. (Guler et al., 2009) investigated on contact performance of oxide reinforced copper composite via mechanical alloying. They had shown samples of 4 wt.% ZnO, 4 wt.% Al_2O_3, 4 wt.% Y_2O_3 reinforced Cu materials, respectively, exhibited both the best conductivity and the best contact performances. Zhu et al. (Zhu et al., 2007) studied on microstructure and performance of electroformed Cu/nano-SiC composite and

reported that nano- SiC embedded in the composite had less impact on electrical property of the composite, which was a benefit to gain Cu matrix composite with both high strength and high electrical conductivity. Liang et al. (Liang et al., 2004) studied on kinetic analysis of Al_2O_3/Cu composite prepared by mechanical milling and gave the effects of soaking time on the electrical conductivity and hardness of Al_2O_3/Cu composite. They reported that with increase in soaking time from 0 to 1 h, the electrical conductivity and hardness of the composite increased and higher hardness value obtained at 1 h. With further prolonged internal oxidation time, the hardness decreased, whereas the electrical conductivity increased appreciably. The results of prolonged internal oxidation time led to the growth of sintering neck that promoted densification slightly. On the other hand, it caused the driving force of the grain growth would exceed the pinning resistance of Al_2O_3 particles and the Cu grain would grow. So it is reasonable that the electrical conductivity increased, and the hardness decreased.

2.6 Consolidation and sintering

To take the advantage of the unique properties of the nanostructured material the nanometer range powder particles have to be consolidated nearer to full theoretical density of the material, i.e. after consolidation nanofeatures should be retained in the densified material. To achieve this we have to restrict the grain growth or coarsening during densification. Therefore, the temperature and time of consolidation are to be restricted at low value. Densification process of conventional micron size powders is well known and that is mainly takes place by grain coarsening. But in case of nanomaterials grain coarsening is to be restricted to keep the nanofeatures. There are various conventional consolidation processes like hot pressing, hot isostatic pressing, hot forging, extrusion etc., but grain coarsening at higher temperature is the only restriction. A number of non-conventional consolidation methods have been applied to nanopowder densification: Microwave sintering, shock or dynamic consolidation, and field assisted sintering, and spark plasma sintering etc.

Clark et al. and Iskander et al. (Clark et al., 2001; Iskander et al., 1996) reported that microwave sintering is very effective in case of ceramics. Microwave sintered achieves full density with lower temperature and shorter times than conventional sintering. It was reported that metallic materials reflect microwave, or microwave cause sparking of metallic materials. But using a susceptor, metallic materials could be sintered to full density. So in the field of metals and alloys, there has been little research on the heating effects of microwave sintering (Roy et al., 1999; Iskander et al., 1999). Anklekar et al. (Anklekar et al., 2001; Anklekar et al., 2005) showed that the mechanical properties of microwave sintered samples were superior to those of conventionally sintered samples. Saitou (Saitou, 2006) studied on microwave sintering of iron, cobalt, nickel, copper and stainless steel powders. They have been reported that microwave radiation promoted the sintering of metal powders, but it did not affect the activation energy for sintering and in case Fe in the fcc region it did not affected by microwave radiation but significantly affected only around A_3 transformation temperature. There are various research have been conducted to know the microwave sintering mechanism and detailed understanding about the nature and distribution of the electromagnetic field inside the microwave cavity, microwave–material interaction, material transformations and heat transfer mechanisms for optimizing the process (Das et al., 2009).

Angerer et al. (Angerer et al., 2005) studied on Spark-plasma-sintering (SPS) of nanostructured titanium carbonitride powders sintered at 1600°C and 1800°C (sintering time = 1 min). They reported that the SPS method is capable of obtaining high densities (~94% of theoretical density) combined with small grain-size than that of the conventional sintered samples obtained from various literatures.

In this present study, attempts to synthesize Cu-Cr and (Cu-Cr)–SiC (4 wt.%) nanocomposites by high energy ball milling for 50 h. The extents of alloying, structural and morphological changes of the milled powders are analyzed by XRD, SEM and Fourier transforms infrared radiation (FTIR) spectrometer. Subsequently, the as milled powders were consolidated using uniaxial pressing followed by cold isostatic pressing (CIP) at 1500 MPa and then sintering using conventional (at 900°C

and 1000°C), vacuum (at 900°C and 1000°C), and microwave sintering (at 800°C and 900°C) techniques. Measurement of physical properties like relative density (using Archimedes principle) and electrical conductivity of all the sintered samples were measured. Mechanical properties, namely, Vickers hardness and wear resistance were also investigated.

CHAPTER 3 Experimental

This chapter deals with the details of the experimental procedures carried out in this investigation. The materials were subjected to a series of characterizations, e.g., microstuctural characterization by X-ray diffraction (XRD), scanning electron microscopy (SEM), Fourier transform infrared radiation (FTIR), atomic force microscopy (AFM) and nano zeta sizer (NZS) analysis, sintering behavior by dilatation study, mechanical properties like Vickers hardness measurement and wear resistance, and electrical properties like conductivity. The details of each process are described in the following sections.

3.1 Development of Cu-based nanocomposites

In the present investigation mechanical milling was carried out for preparation of 4 compositions, namely, $Cu_{99}Cr_1$, $Cu_{94}Cr_6$, $Cu_{99}Cr_1$–4 wt.% SiC, and $Cu_{94}Cr_6$–4 wt.% SiC. Milling was in two different milling media, i.e., WC milling media for preparation of nanosize SiC and stainless steel milling media for Cu-based nanocomposites. The details are described below.

3.1.1 Mechanical milling

The elemental powders of Cu, Cr (purity >99.0 %) were used to blend the compositions $Cu_{99}Cr_1$, $Cu_{94}Cr_6$, $Cu_{99}Cr_1$–4 wt.% SiC, and $Cu_{94}Cr_6$–4 wt.% SiC under protective atmosphere. These were subjected to high energy milling in the stainless-steel grinding media at a mill speed of 400 r.p.m. by means of a Fritsch Pulverisette-5 planetary ball mill. The ball to powder weight ratio was 10:1. Toluene was used as the process control agent. Before this, laboratory grade SiC powder (purity >96.0%) were initially ball milled at 300 r.p.m. for 16 h in a WC grinding media to prepare nanosize (~30 nm) powder particles. Powder samples were collected after 30 min, 2 h, 5 h, 10 h, 20 h, 35 h and 50 h of milling for XRD, SEM and FTIR.

Fig. 3.1: Fritsch Pulverisette-5 planetary ball used for mechanical milling.

3.1.2 Consolidation of milled powder

Uniaxial pressing followed by cold isostatic pressing were carried out at an applied pressure of 1500 MPa to consolidate the 50 h milled powder samples. The relative green densities were measured which gave similar level of densification for all the compositions. The compacts were sintered by three consolidation techniques, conventional pressure-less method at 900°C and 1000°C for 1 h soaking period under a flowing argon atmosphere, vacuum sintering at 900°C and 1000°C for 1 h and microwave sintering at 800°C and 900°C for 30 min using 2.45 GHz frequency and a power of ~900 W.

3.2 Microstructural characterization

3.2.1 X-ray Diffraction (XRD)

The phase evolution at different stages of mechanical milling were studied by XRD analysis using the Cu K_α (λ=1.542Å) in a Philips X-pert MPD X-ray diffractometer. X-Ray diffraction patterns were recorded from 20˚ to 100˚ with an accelerating voltage of 40 kV. Data were collected with a counting rate of 2˚/min. The average crystallite size of

Cu rich nano composite was determined from the broadening of Cu reflection after stripping of $K\alpha_2$ component using Scherrer calculator. For the overlapping peaks, the full-width at half intensity maximum and the true Bragg angle (2θ) were determined by an appropriate deconvolution exercise. The lattice parameter of Cu-based solid solutions (a) was calculated from the peak positions in the XRD pattern by extrapolation of a against ($\cos^2\theta/\sin\theta$) plot to $\cos\theta = 0$.

Fig. 3.2: Philips X-pert MPD X-ray diffractometer.

3.2.2 Scanning Electron Microscopy (SEM)

A JEOL JSM-6480 LV scanning electron microscope (Fig. 3.3) was used for the morphology, particle size and microstructural characterization of different hours milled powder and sintered specimens. Micrographs are taken at suitable accelerating voltages for the best possible resolution using the secondary electron imaging.

Fig. 3.3: JEOL JSM-6480LV scanning electron microscope.

3.2.3 Atomic Force Microscopy (AFM)

VEECO di Innova atomic force microscope was utilized to study AFM micrograph of few sintered samples. In the present investigation this instrument is mainly used for found out the average particle size of conventional sintered specimens.

Fig. 3.4: VEECO di Innova atomic force microscope.

3.2.4 Nano zeta sizer

The particle size of the milled powder was measured in Nano zeta sizer (Nano ZS, Malvern). The sample was prepared by dispersing a small amount of powder in de-ionized water with constant ultrasonic vibration and magnetic stirring for 30 minutes each. Then the sample was kept in a sample holder with the help of syringe and analyzed.

Fig. 3.5: Nano ZS (Malvern), Nano zeta sizer used in the present study.

3.2.5 Fourier Transform Infrared Radiation (FTIR) spectroscopy

The percentage of transmission of Infrared Radiation was measured by Fourier transforms infrared radiation (FTIR) spectrometer (Perkin-Elmer Spectrum RXI). A small amount of potassium bromide (KBr) was mixed with powder sample and then it was pressed to prepare pellets. The pellet was kept in a sample holder of FTIR spectrometer and analyzed to get results.

Fig. 3.6: Perkin-Elmer Spectrum RXI, Fourier transforms infrared radiation (FTIR) Spectrometer.

3.2.6 Dilatometry

NETZSCH DIL 402C Dilatometer was used to investigate the sintering characteristics and diffusion behavior of the 50 h milled samples. The expansion or contraction behavior of solid specimen was studied by heating it up to 950ºC with a heating rate of 5ºC/min under inert argon atmosphere (impurity <10 ppm).

Fig. 3.7: NETZSCH DIL 402C Dilatometer.

3.3 Evaluation of Mechanical Properties

3.3.1 Vickers Hardness Measurement

Vickers hardness tester (Leco LV 700) was used to determine Vickers hardness values of all the sintered specimens using 1 kg load for a dwell time of 40 s. The variation in the hardness values obtained for a particular specimen was ±4 Hv.

Fig. 3.8: Leco LV 700 Vickers hardness tester

3.3.2 Evaluation of Wear Resistance

In the present study Ball-On-Plate Wear Tester TR-208 M1 instrument was used to determine the wear behavior of the microwave sintered samples. This experiment was done under a constant load of 5N for 300 S at 15 rpm.

Fig. 3.9: Ball-On-Plate Wear Tester TR-208 M1.

3.4 Evaluation of Electrical Conductivity

The electrical conductivity of all the sintered samples was investigated by 4-probe method in SIGMATEST D 2.068, FOERSTER instrument. The conductivity was as per the International Annealed Copper Standard (IACS) (100%).

Experimental details are shown in the flow diagram below:

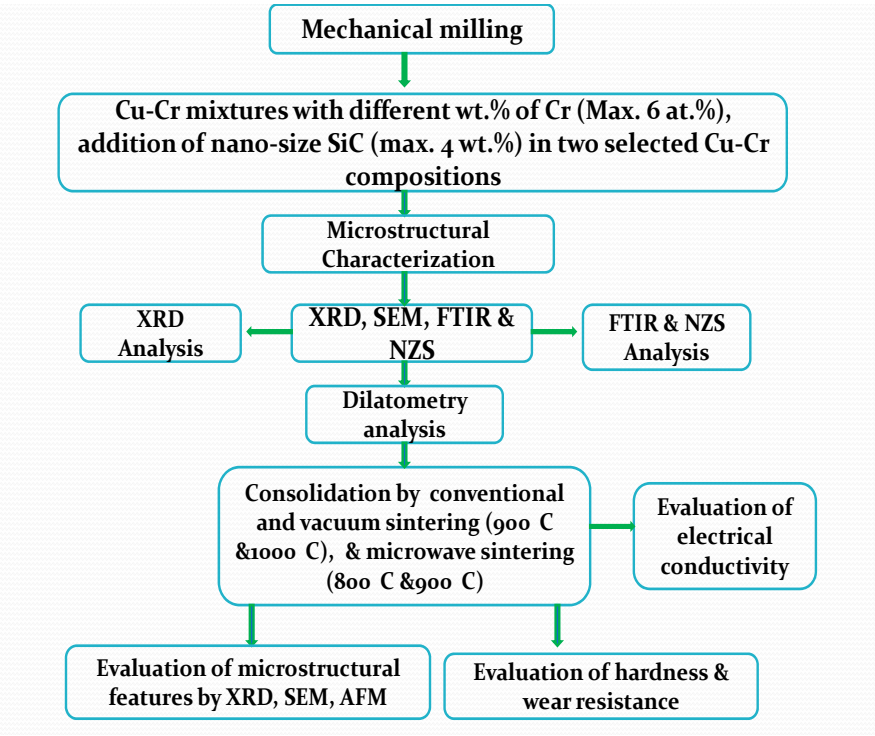

CHAPTER 4 Results and Discussion

4.1 Structural Characterization of Milled Samples

The structural characterizations of the mechanically milled powder samples were carried out by SEM, XRD, FTIR and dilatation analysis.

4.1.1 SEM analysis

SEM micrographs in Fig. 4.1(a-c) show gradual refinement of ball milled $Cu_{99}Cr_1$ powder particles with progress of milling for (a) 30 min, (b) 10 h and (c) 50 h. After 30 min of milling the powders show layered and non uniform structure (Fig. 4.1(a)), which is the characteristics feature of mechanical milling of ductile-brittle combinations of powder particles for the initial stage of milling. Upon further milling up to 50 h, the layered structure gradually refined as fracture predominates over cold welding.

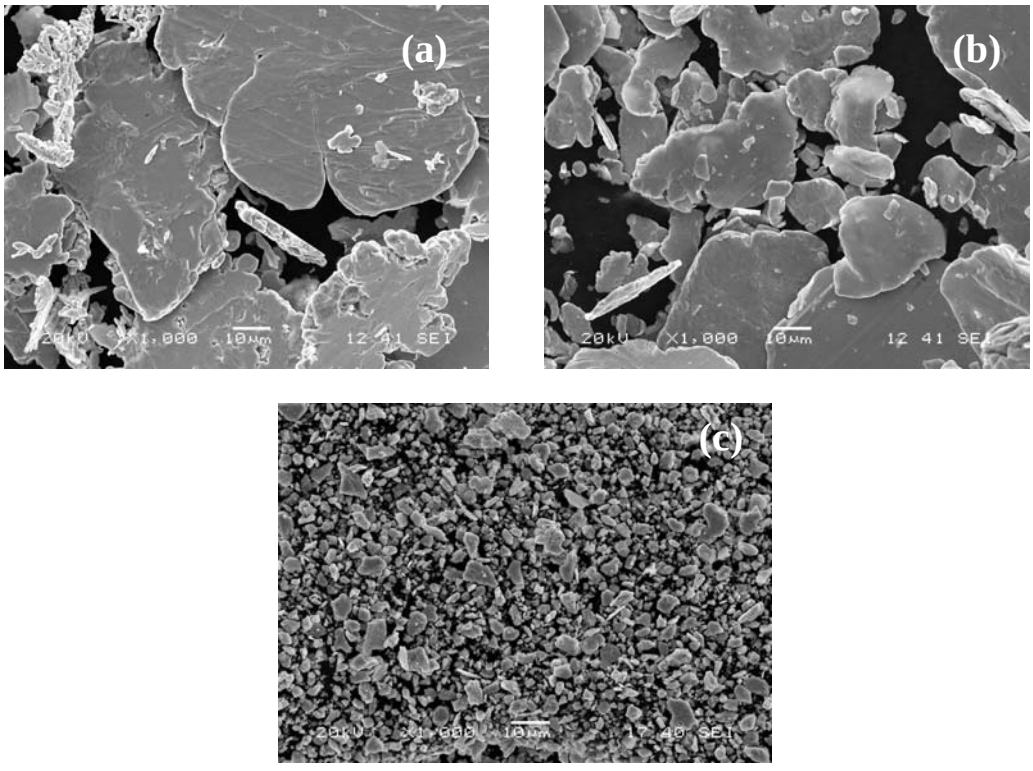

Fig. 4.1: SEM micrographs of $Cu_{99}Cr_1$ powder particles milled for (a) 30 min, (b) 10 h and (c) 50 h, respectively.

The sub-micron sized particles seemed to be agglomerated which is clearly distinguishable from SEM micrograph as shown in Fig. 4.1(c). The similar trend of changes in the morphology was observed for all other compositions studied in the present investigation.

4.1.2 XRD analysis

Figure 4.2 shows XRD patterns of 16 h milled powder sample milled in WC grinding media. From the phase analysis it has been found that peak intensity much reduced from initial, without milled powder and peak broadening occur. With SiC peaks SiO_2 are also visible. This is mainly due to impurity content in SiC (purity >96%). Analysis of the XRD data revealed that average crystallite size of the milled powder was ~30 nm.

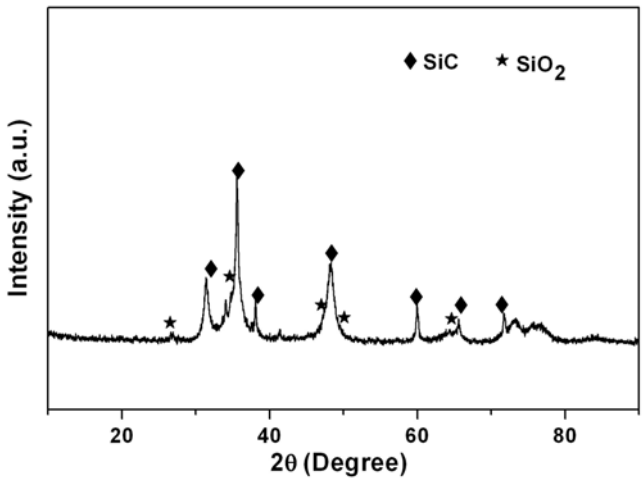

Fig. 4.2: XRD pattern of 16 h milled SiC powder sample.

Figures 4.3(a-d) show the modulation of the XRD patterns of $Cu_{99}Cr_1$, $Cu_{94}Cr_6$, $Cu_{94}Cr_6$–4 wt.% SiC and $Cu_{99}Cr_1$–4 wt.% SiC compositions with the progress of milling up to 50 h. It is interesting to note that Cu and Cr peaks are clearly visible after 50 h of milling. It is to be noted that the peak intensity gradually decreased and broaden with progress of milling in all the cases. But, broadening of peaks and decrease in the intensity was found to be higher in case of $Cu_{99}Cr_1$–4 wt.% SiC and $Cu_{94}Cr_6$–4 wt.% SiC compared to composition without SiC reinforcement. This is

probably due to the faster reduction of particle size because of the presence of the harder, brittle SiC particles in the blend.

A few small peaks corresponding to $Cr_{23}C_6$ and Fe_2C phases were detectable from the 50 h milled sample of $Cu_{99}Cr_1$ composition, which is shown in Fig. 4.3(a). The carbon contamination was occurred possibly due to from toluene, which was used as a process control agent during milling. In case of $Cu_{94}Cr_6$ (Fig. 4.3(b)), a few small peaks corresponds to Cr_3C_2 are visible along with the peaks of Cu, Cr and Fe. The peaks corresponding to Fe are possibly due to the contamination from milling container.

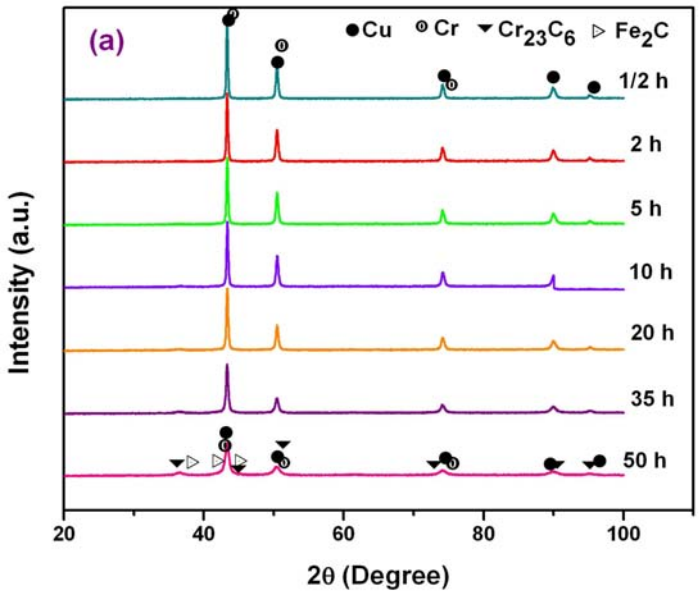

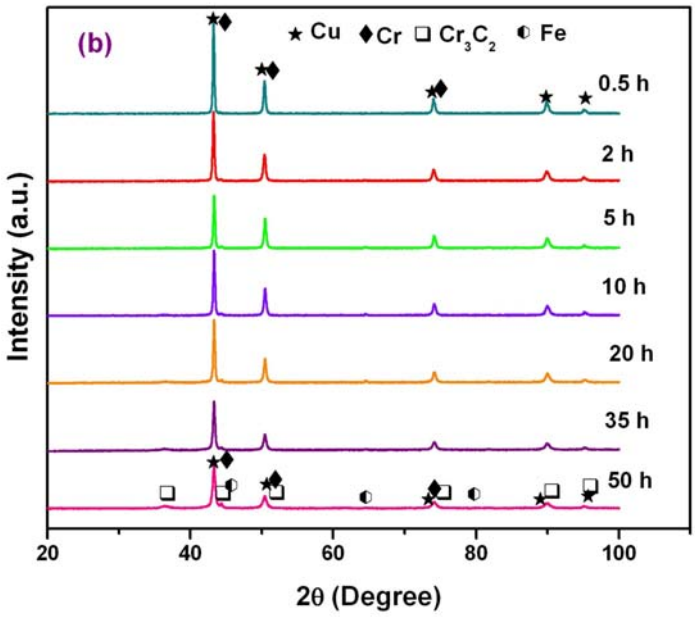

Fig: 4.3: XRD pattern of (a) $Cu_{99}Cr_1$ and (b) $Cu_{94}Cr_6$ nanocomposites powder samples during milling.

Analysis of $Cu_{99}Cr_1$–4 wt.% SiC composition, showed the presence of SiC, $CrSi_2$ and $Cr_{23}C_6$ phases after 2 h of milling (Fig. 4.3(c)). After 20 h of milling, SiC, CrSi, $CrSi_2$ and $Cr_{23}C_6$ phases are observed. CrSi and $Cr_{23}C_6$ were gradually disappeared after MA of 20 h. No peaks corresponding to these phases were detectable by XRD analysis after 50 h of milling, whereas, SiC and $CrSi_2$ phases were still persisted as shown in Fig. 4.3(c). The formation of CrSi, $CrSi_2$ and $Cr_{23}C_6$ phases were possibly due to the reaction of elemental Cr with the contaminants from milling media and impure SiC, i.e., C from toluene, and Si from impure SiC.

From XRD analysis of $Cu_{94}Cr_6$–4 wt.% SiC as shown in Fig. 4.3(d) Cu and Cr peaks are visible from initial stage to 50 h of milling. $CrSi_2$ and Si_5C_3 phases were detected after 50 h of milling only. The peak broadening and decrease in peak intensity is maximum for this composition compared to all other compositions, because of presence of higher percentage of Cr along with 4 wt.% SiC phases.

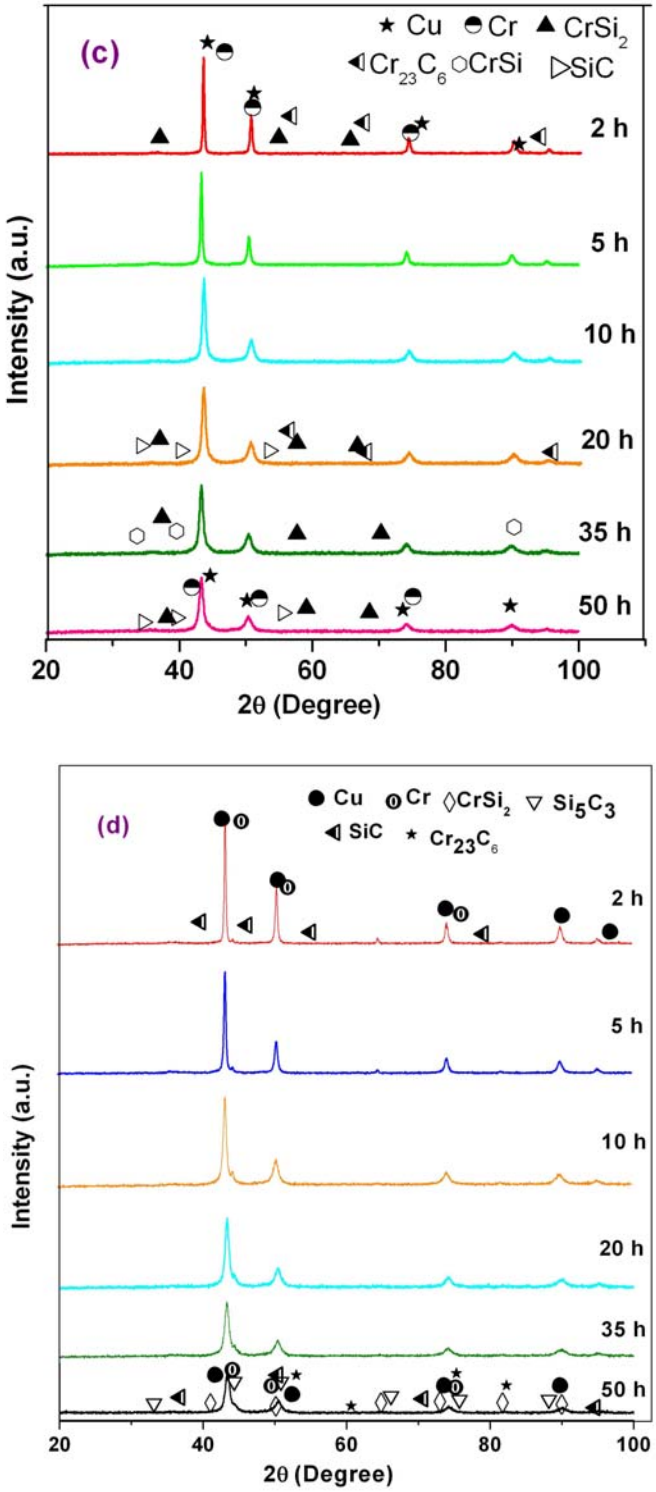

Fig: 4.3: XRD pattern of (c) $Cu_{99}Cr_1$–4 wt.% SiC and (d) $Cu_{94}Cr_6$–4 wt.% SiC nanocomposites powder samples during milling.

The stability of any new phase(s) formed/disappeared during continued deformation depends on kinetic factors and the structural factors like the extent of crystallite size refinement, lattice strain developed etc. (Mula et al., 2008). The possible reasons of the phase evolution in the Cu-Cr and Cu-Cr–SiC systems by mechanical milling could be analyzed in the light of Hume-Rothery's rules of alloying. The atomic radii of Cr (0.1249 nm) and Si (1.17 nm) which are lower than that of Cu (1.275 nm) (Brandes et al., 1992). Here, the atomic size differences are within 15 % of the atomic radius of Cu. So it is expected that smaller size Cr and Si could enter into the solid solution of Cu. The solubility of Cr in Cu is less than 0.03% (at.%) at 400°C as per the equilibrium phase diagram (Liu et al., 2004). But, the solid solubility of solute element can be extended by high energy ball milling (Suryanarayana, 2001). Therefore, analysis of the XRD data has been carried out to find out whether Cu-Cr solid solution was formed during milling up to 50 h.

The XRD data were analyzed for crystallite size refinement, lattice microstrain(%) and lattice parameter variation of Cu based solid solution of all the compositions. The crystallite size gradually decreases with progress of milling which was clearly visible in Fig. 4.4. Up to 20 h of milling rapid decrease in crystallite size can be noticed from the figure. After that a very slow trend in crystallite size refinement is observed. The refinement of crystallite size is much more prominent in case of composition having SiC compared to that of $Cu_{99}Cr_1$ and $Cu_{94}Cr_6$ compositions for the same duration of milling. This could be corroborated with the XRD peak broadening and reduction peak intensity of the same composition (Figs. 4.3). In case of $Cu_{99}Cr_1$ composition after 50 h of milling, crystallite size was found to be in the range of 18–22 nm, whereas, it was in the range of 14–16 nm for $Cu_{99}Cr_1$–4 wt.% SiC.

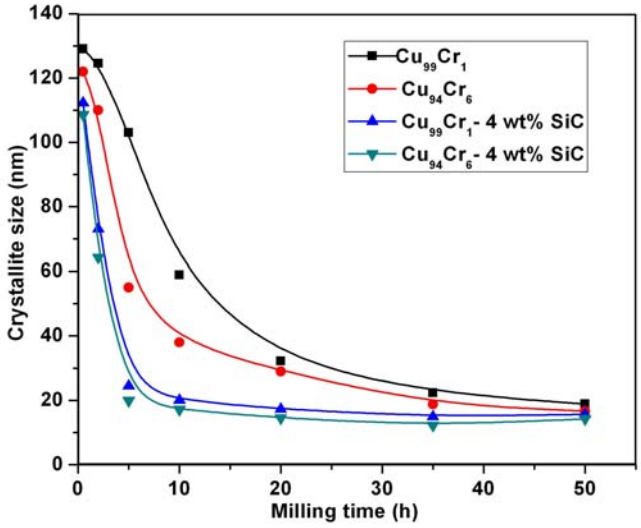

Fig. 4.4: Variation of crystallite size of different compositions with milling time.

From Fig. 4.5 it is observed that with increase in milling time the lattice microstrain (%) gradually increases rapidly up to 35 h of milling and after that it increases slowly and attains almost a constant value up to 50 h of milling. Due to the presence of harder and brittle SiC particles in $Cu_{99}Cr_1$–4 wt.% SiC and $Cu_{94}Cr_6$–4 wt.% SiC, crystallite size were found to be much finer (as shown in Fig. 4.4), which increases the lattice microstrain(%) to higher value than that of $Cu_{99}Cr_1$ and $Cu_{94}Cr_6$ compositions. The lattice microstrain(%) is in the range of 0.5–0.55 % after 50 h of milling in case of Cu-Cr and in case of compositions containing SiC, it is in the range of 0.56–0.7 %.

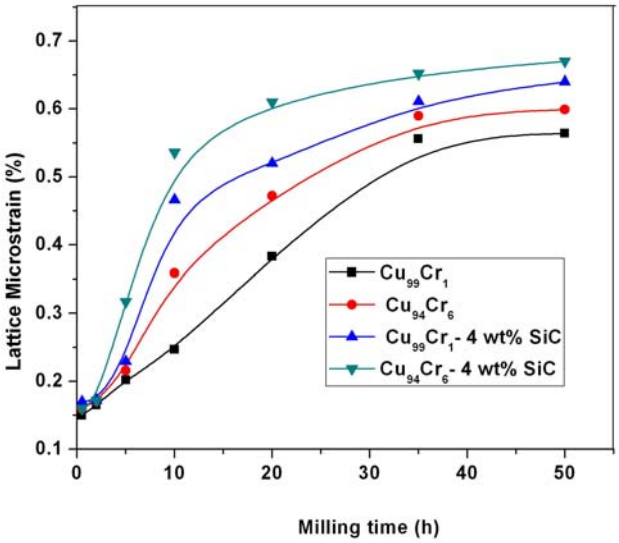

Fig. 4.5: Variation in lattice microstrain(%) of different compositions with milling time.

Fig. 4.6 shows the variation of lattice parameters of Cu based solid solutions with progress of milling of $Cu_{99}Cr_{1,}$ $Cu_{94}Cr_6$, $Cu_{99}Cr_1$–4 wt.% SiC and $Cu_{94}Cr_6$–4 wt.% SiC compositions up to 50 h. In all cases a little decrease in lattice parameter was observed up to 20 h of milling. After that there is no variation of lattice parameter was observed with further milling. The decrease in lattice parameter was possibly due to the formation of solid solution of Cr in Cu. As per the equilibrium phase diagram the solubility of Cr in Cu is less than 0.03% (at.%) at 400°C (Liu et al., 2004). In the present investigation also, it was observed that solid solubility of Cr in Cu is less than 1 at.% (Fig. 4.3(a)). With increase in Cr content in Cu, variation in solid solubility of Cr in Cu was not detected, which is possibly reflected from the constant lattice parameter of the Cu-based solid solutions after 20 h of milling in all the composition. After 20 h milling, the alloying element either forms compounds with impurities from milling media or retains as mechanical mixture like SiC. Alloying element, when does not enter into solid solution, do not contribute to the lattice parameter variation of the Cu-based solid solution during milling.

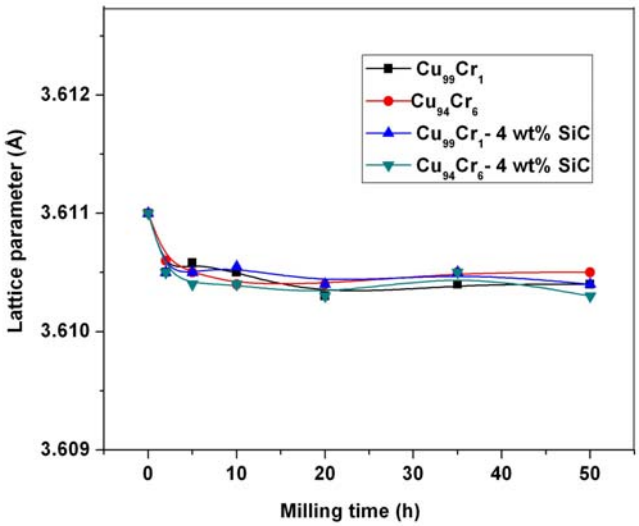

Fig. 4.6: Variation of lattice parameter of Cu-based solid solutions with milling time.

4.1.3 FTIR analysis

Fig: 4.7(a) shows the Fourier transforms infrared radiation (FTIR) spectrometer plot of $Cu_{99}Cr_1$ milled for different durations along with that of $Cu_{99}Cr_1$–4 wt.% SiC and $Cu_{94}Cr_6$–4 wt.% SiC milled for 50 h. It is evident from the figure that as the milling time progresses (%)transmittance is getting decreased. It is due to the increase in total surface area due to decrease in particle size with progress of milling. 50 h milled of SiC composition shows much lower value of (%)transmittance than that of without SiC composition milled for same duration. From this, it was also found that crystallite size was much finer in case of SiC composition, which was confirmed by crystallite size (Fig. 4.4) analysis of XRD patterns.

The calculated crystallite size from the XRD patterns of milled samples of different duration has been plotted against the (%)transmittance obtained from FTIR analysis of the same sample and is shown in Fig: 4.7(b). It is evident from the figure that the percentage of transmittance is decreasing with decrease in the crystallite size.

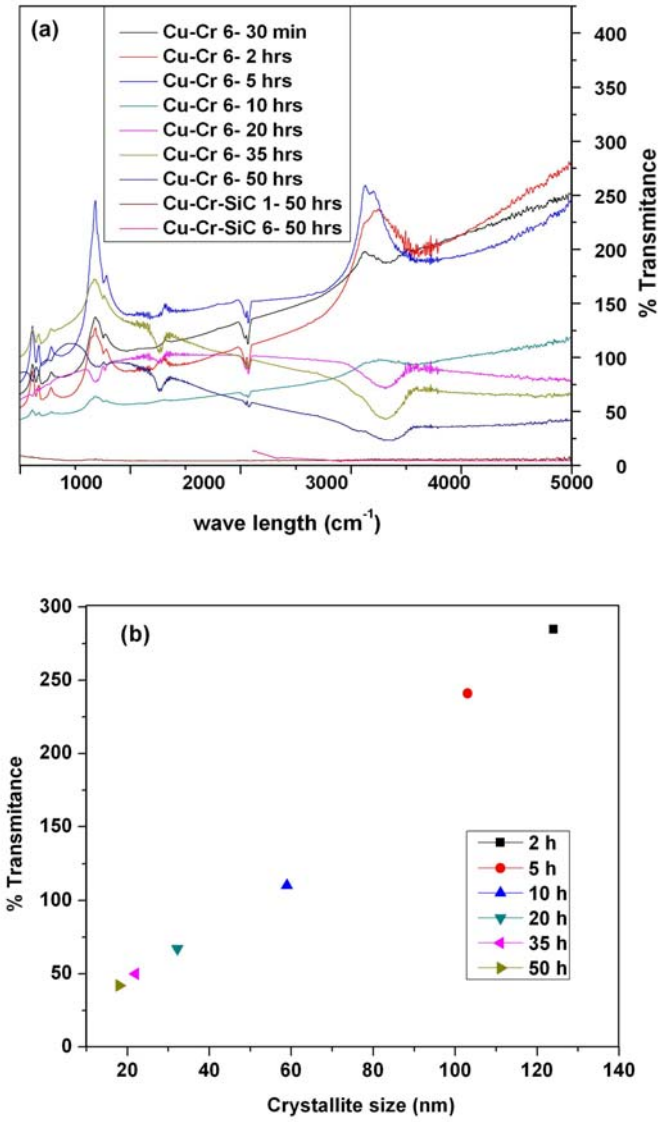

Fig. 4.7: (a) FTIR plot of $Cu_{99}Cr_1$ milled for different durations along with that of 50 h milled $Cu_{99}Cr_1$–4 wt.% SiC and $Cu_{94}Cr_6$–4 wt.% SiC compositions. (b) %Transmittance vs. crystallite size of Cu-based solid solution of $Cu_{99}Cr_1$ composition with reduction of crystallite size.

4.1.4 Particle size analysis

Particle size distribution of the 50 h milled samples was analyzed by nano zeta sizer (Nano ZS, Malvern) and is shown in Fig. 4.8(a-d). It is evident from the statistical figures that particle size distribution was reduced from 120–250 nm to 105–190 nm

with increasing Cr content from $Cu_{99}Cr_1$ to $Cu_{94}Cr_6$, and it was further reduced to much finer size 80–170 nm for $Cu_{99}Cr_1$–4 wt.% SiC and 50–150 nm for $Cu_{94}Cr_6$–4 wt.% SiC) when hard SiC particles were added with the Cu-Cr compositions for the same duration of milling (50 h) under same milling conditions. This clearly indicates that addition of harder element/particles with soft matrix decreases the particles size and its distribution to a narrower range for the same duration of milling. This is because the softer matrix is getting strained faster by plastic deformation when hard brittle material is added (Suryanarayana, 2001).

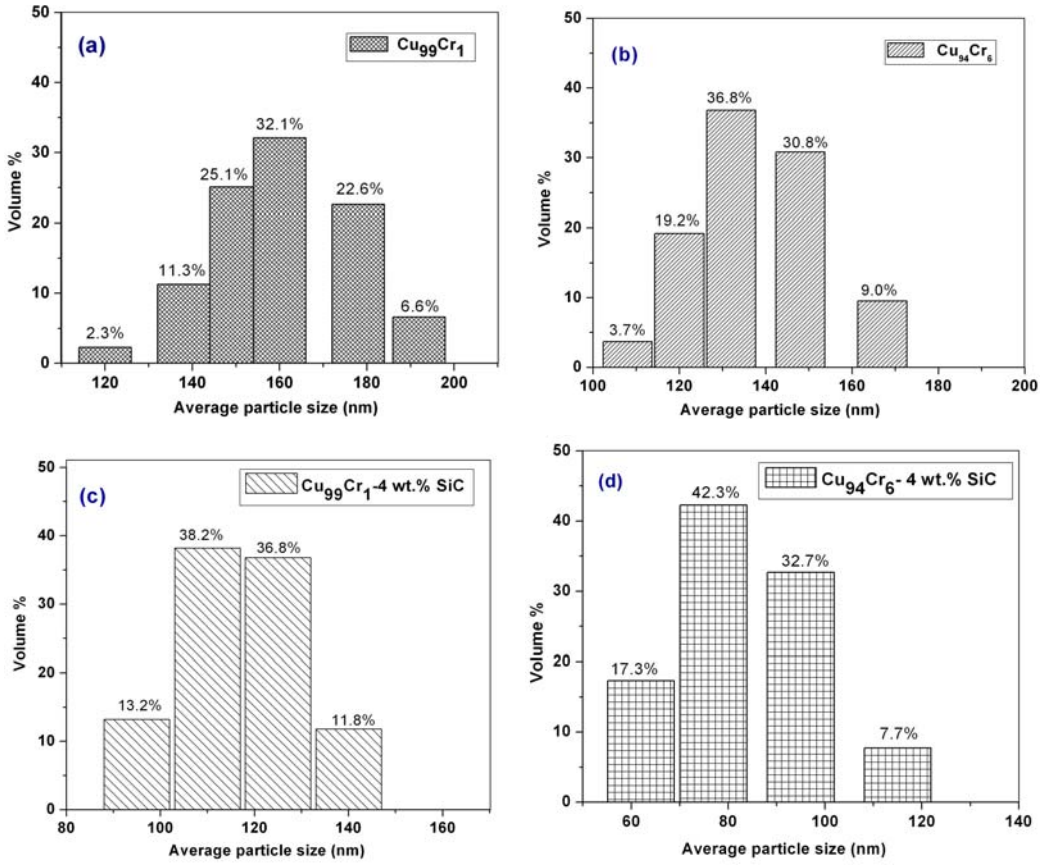

Fig. 4.8: Variation of average particle size with volume % of that for (a) $Cu_{99}Cr_1$, (b) $Cu_{94}Cr_6$, (c) $Cu_{99}Cr_1$–4 wt.% SiC, (d) $Cu_{94}Cr_6$–4 wt.% SiC compositions.

4.2 Consolidation and sintering

50 h milled samples of all the compositions were uniaxially pressed with an applied pressure of 1500 MPa. To increase green density of compacts, cold isostatic pressing

were also carried out with the applied pressure of 1500 MPa, which increased the density of green compact by 2–3 %. It is known that compare to conventional sintering technique application of other non conventional sintering methods can give better mechanical properties to the metal matrix composites (Eckert, 2002). With a view to produce bulk samples for the evaluation of mechanical properties and to characterize the related microstructural features, the compacts were sintered by different methods, viz., conventional sintering (at 900ºC and 1000ºC under argon atmosphere for 1 h soaking period), vacuum sintering (at 900ºC and 1000ºC for 1 h) and microwave sintering (at 800ºC and 900ºC for 30 min duration). Microwave sintering was carried out using 2.45 GHz frequency and a power of ~900 W.

4.2.1 Dilatation and diffusion

To investigate the sintering characteristics and diffusion behavior of the milled samples, the thermal dilatation measurement was carried out using NETZSCH DIL 402C instrument. It is a useful method to determine sintering temperature of any unknown materials. The expansion or contraction behavior of solid specimen was studied by heating it up to 950ºC with a heating rate of 5ºC/min under inert argon atmosphere (impurity <10 ppm). Fig. 4.9 shows dilatation behavior of 50 h milled sample of $Cu_{94}Cr_6$ composition as a function of temperature. Initially, it is observed that there is an expansion in the specimen up to ~700°C possibly due to thermal expansion of the material and just after that there is a sharp decrease in the curve indicating rapid contraction in the volume, which is due to onset of diffusion of nanoparticles and decrease in the porosity in the specimen. Therefore, the dilatation measurement (in Fig. 4.9) indicates that sintering of the mechanically milled specimens above 700°C can generate bulk consolidated products.

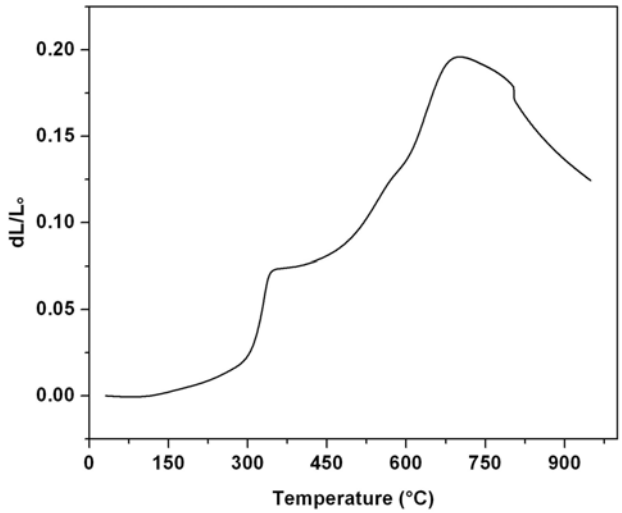

Fig. 4.9: Dilatation behavior of 50 h milled $Cu_{94}Cr_6$ specimen with increasing temperature up to 950°C.

4.2.2 Microstructural investigation of the sintered specimens

The microstructural features of conventional pressure-less sintered, vacuum sintered and microwave sintered specimens were characterized by SEM, XRD and AFM. Table 4.1 summarizes the percentage densification obtained by different sintering methods at different temperatures. Conventional pressure-less sintering at 900°C for 1 h under argon atmosphere resulted in lower densification (relative density 78–84%) for all the compositions. Sintered density was increased by 4–5%, when sintering temperature was raised to 1000°C. Sintering carried out under vacuum at 900°C and 1000°C for 1 h also led to similar level of densification compared to the conventional sintering. On the other hand, remarkable improvement in sintered density was achieved by microwave sintering at 800°C and 900°C only for 30 min soaking period, and highest sintered density was measured ~95% at 900°C. It was observed that microwave sintering is the most effective compared to the other consolidation methods used in the present investigation.

Conventional and vacuum sintering of $Cu_{99}Cr_1$ resulted 5–11% increase in the sintered density, whereas, for microwave sintering it was 17–19%, compared to the green density of the specimens. With increase in Cr percentage, i.e., for $Cu_{99}Cr_1$ and $Cu_{94}Cr_6$ composition, almost similar level of densification was observed for

conventional and vacuum sintering. A much higher level of densification (increase in the sintered density 17–19% compared to green density) was resulted for the same composition using microwave sintering technique. When 4 wt.% of SiC (~30 nm) was added to the Cu-Cr blends, the variation in densification was found to be much more prominent. The maximum green density achieved using same level of uniaxial pressure (1500 MPa) was ~75% for the composition containing SiC, compared to that of Cu-Cr blends (~80%). This is due to the presence of hard, non deformable SiC particles, which hinder the plastic deformation during pressing. Conventional and vacuum sintering of SiC containing compositions resulted almost similar level of densification at 900°C and 1000°C; but, it is clearly demarcated that densification level is much less than the densification of Cu-Cr compositions without SiC at the same temperatures.

Microwave sintering is found to be very much effective in densification of specimens containing ceramic material (SiC) compared to the that of metallic materials only (Cu-Cr blends). In case of $Cu_{99}Cr_1$–4 wt.% SiC and $Cu_{94}Cr_6$–4 wt.% SiC compositions, increase in the sintered density was measured to be 20–24%, compared to that of green density of the compacts, whereas, it was 17–19% in case of Cu-Cr alloys only at the same sintering temperatures using same technique.

It can be concluded that microwave sintering technique is found to be most effective in consolidation of Cu-Cr and Cu-Cr–SiC nanocomposites. As microwave sintering requires less sintering temperature and less soaking period compare to conventional or vacuum sintering, it is possible to produce bulk size nanocomposites without much grain coarsening (Oghbaei et al., 2010). The sintered density can be further increased to above 95% if non conventional sintering techniques, namely, spark plasma sintering (SPS), high pressure torsion etc. are employed (Kwon et al., 2006). So that the mechanical properties like strength, hardness, wear resistance and electrical properties could be enhanced to desired level.

Table 4.1: Relative sintered density of $Cu_{99}Cr_1$, $Cu_{94}Cr_6$, $Cu_{99}Cr_1$–4 wt.% SiC and $Cu_{94}Cr_6$–4 wt.% SiC compositions, conventionally sintered at 900°C and 1000°C, vacuum sintered at 900°C and 1000°C, microwave sintered at 800°C and 900°C.

Blend Composition	Green Density (%)	Sintered Density (%)					
		Conventional sintering		Vacuum sintering		Microwave sintering	
		900°C	1000°C	900°C	1000°C	800°C	900°C
$Cu_{99}Cr_1$	80	84	87	85.5	89	93.7	95
$Cu_{99}Cr_1$–4 wt.% SiC	75	78.5	82	79	82.5	92	93.2
$Cu_{94}Cr_6$	80	83.5	85.5	84.5	86	93.6	94.3
$Cu_{94}Cr_6$–4 wt.% SiC	74.8	78	82.3	79	82.4	90	90.8

SEM analysis of sintered specimens

The microstructures of polished sintered samples were taken using (JEOL JSM-6480 LV) scanning electron microscope. Figs. 4.10(a-d) compare the microstructures of $Cu_{94}Cr_6$ and $Cu_{94}Cr_6$–4 wt.% SiC compositions sintered at 900°C by conventional and microwave sintering techniques. Clearly, microwave sintered samples showed less amount of porosity and significantly lower grain coarsening than that of conventionally sintered specimens. This can be evidenced from relative density also as shown in Table 4.1. Better grain distribution and uniform grain size with less porosity in microwave sintered specimen is expected to provide better combination of mechanical properties (like hardness and wear resistance) and electrical conductivity.

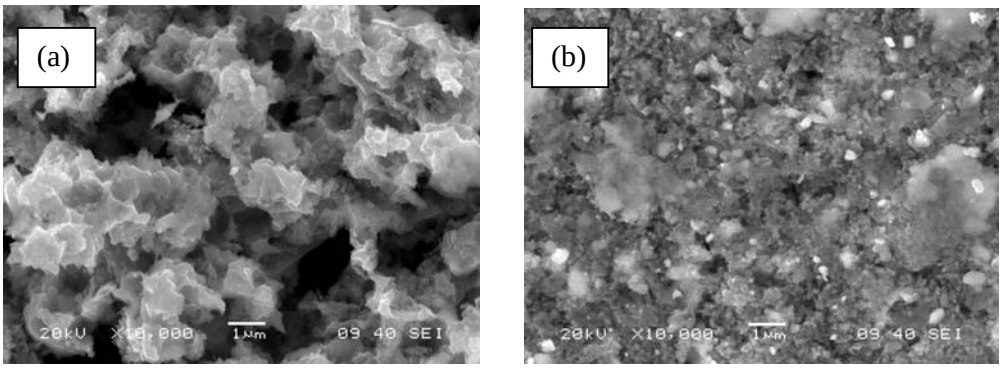

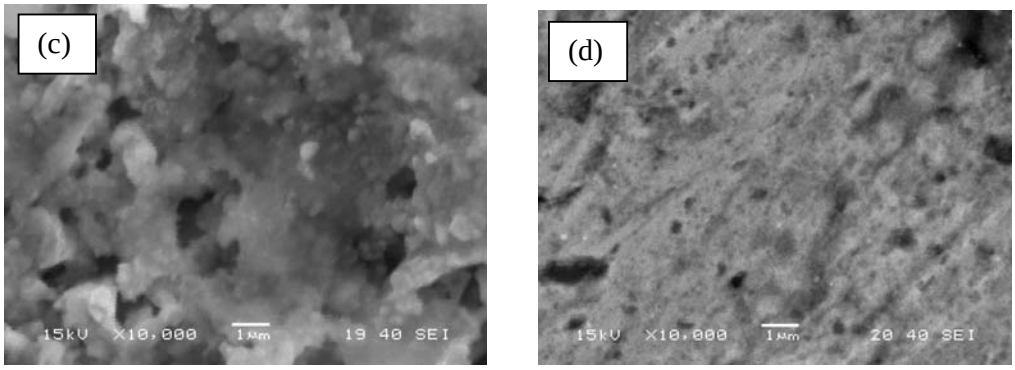

Fig. 4.10: SEM micrographs of conventionally sintered ((a), (b)) and microwave sintered samples ((c), (d)) of $Cu_{94}Cr_6$ and $Cu_{94}Cr_6$–4 wt.% SiC sintered at 900°C.

XRD analysis of sintered specimens

Figures 4.11(a-b)–4.13(a-b) show the XRD patterns and phase analysis of four compositions sintered by different techniques at different temperatures. From phase analysis of all the sintered samples revealed that Cu, Cr peaks are much more prominent compared to that of the corresponding 50 h milled samples. Some less intense oxides peaks corresponding to CuO_2, CuO, Si_2O, $Cu(CrO_2)$, and Cr_2O_3 were also visible in XRD patterns of the sintered specimens. This is due to the reaction with residual oxygen present in argon in conventional sintering, O_2 present in vacuum sintering and O_2 present in the furnace atmosphere during microwave sintering.

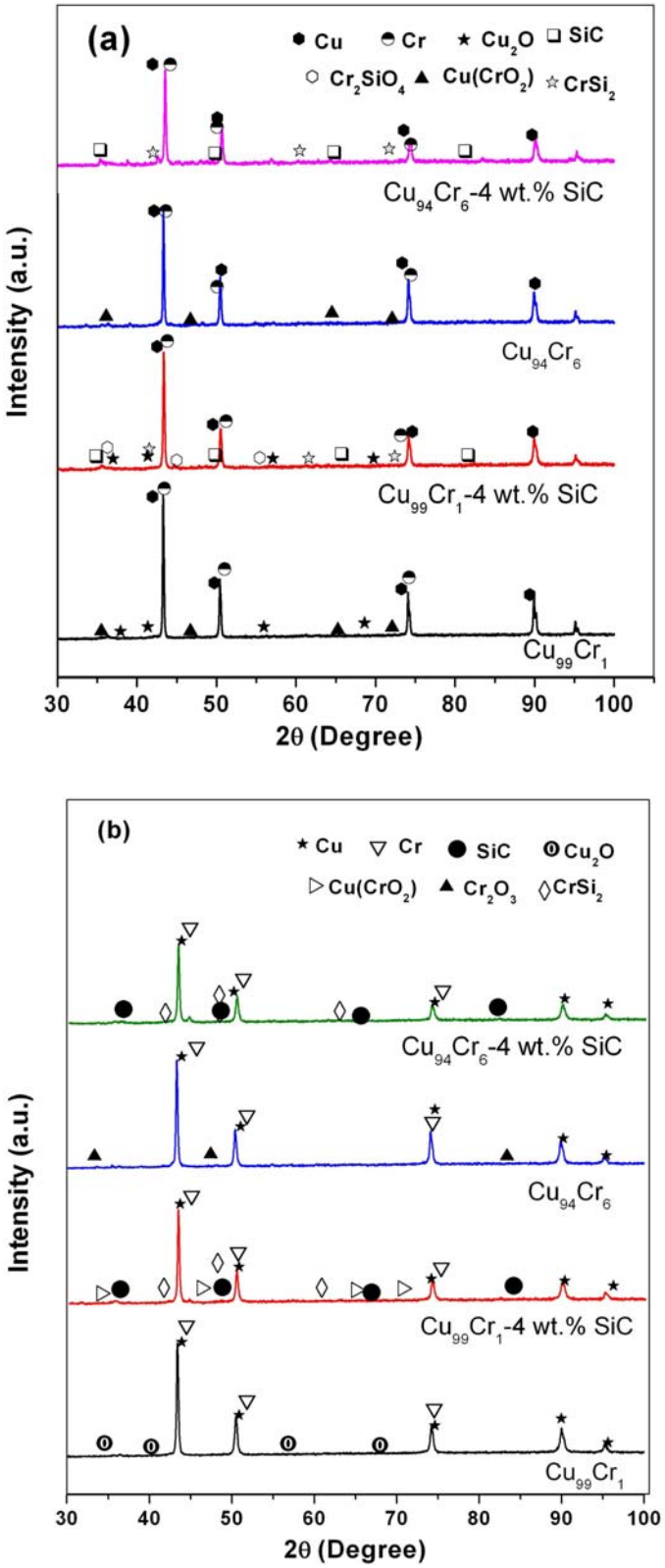

Fig. 4.11: XRD patterns of specimens conventionally sintered at (a) 900°C and (b) 1000°C.

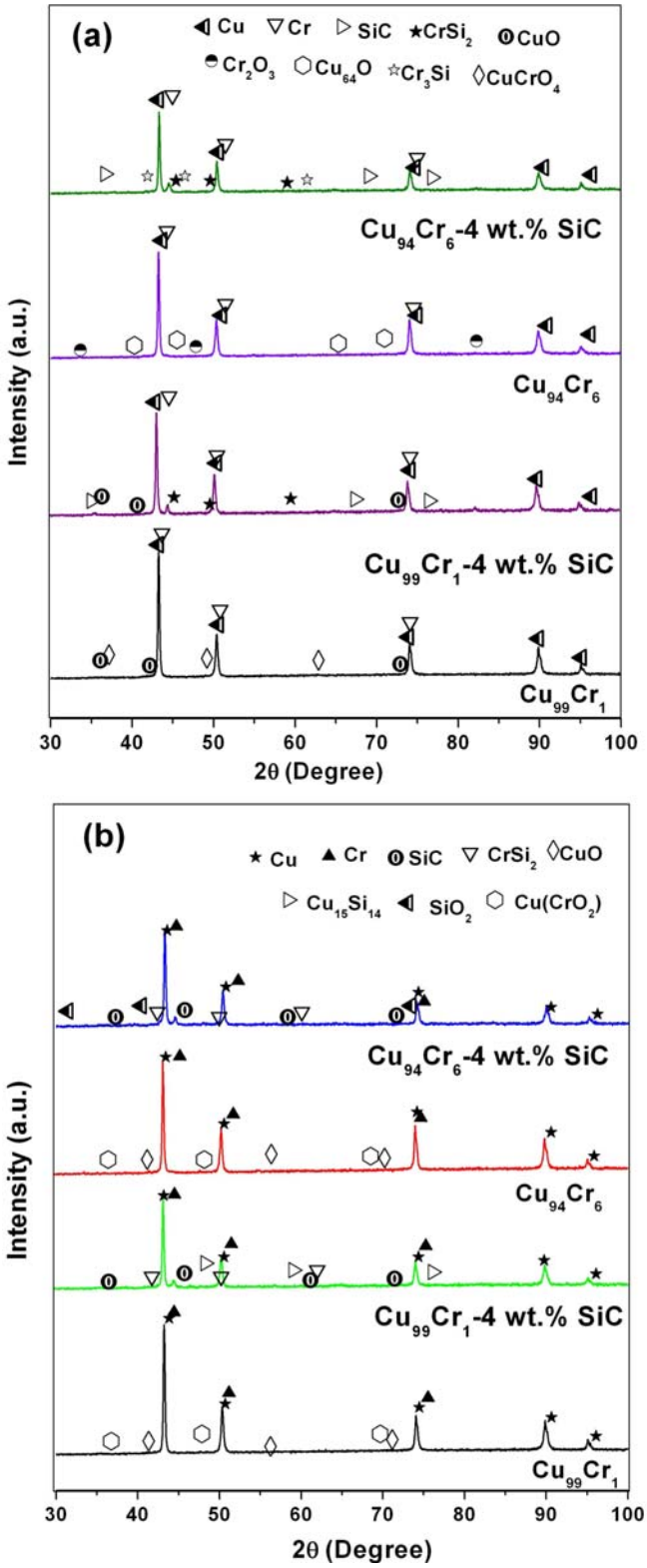

Fig. 4.12: XRD patterns of specimens sintered by vacuum sintering technique at (a) 900°C and (b) 1000°C.

From XRD patterns, it was observed that in case of sintered specimen, peaks became much sharper than that of 50 h milled sample. But if peak intensities of only sintered samples are compared then intensity is very less in microwave sintered specimens (Figs. 4.13(a-b)) than that of the conventional sintered and vacuum sintered samples at the same sintering temperature. Moreover, the corresponding peak intensity is less in case $Cu_{94}Cr_6$–4 wt.% SiC than that of other compositions at the same sintering temperature, possibly because of hindering of grain growth by fine SiC and more amount of Cr particles present in the matrix during sintering.

Along with some oxide peaks, peaks corresponding to $CrSi_2$, Cr_3Si, CrSi and $Cu_{16}Si_{14}$ were also visible in all the sintered samples of the compositions containing SiC, possibly because of presence of highly reactive Si impurities in the added SiC powder. SiC peaks were visible along with Cu and Cr peaks in all SiC reinforced composites indicates the presence of SiC throughout the matrix.

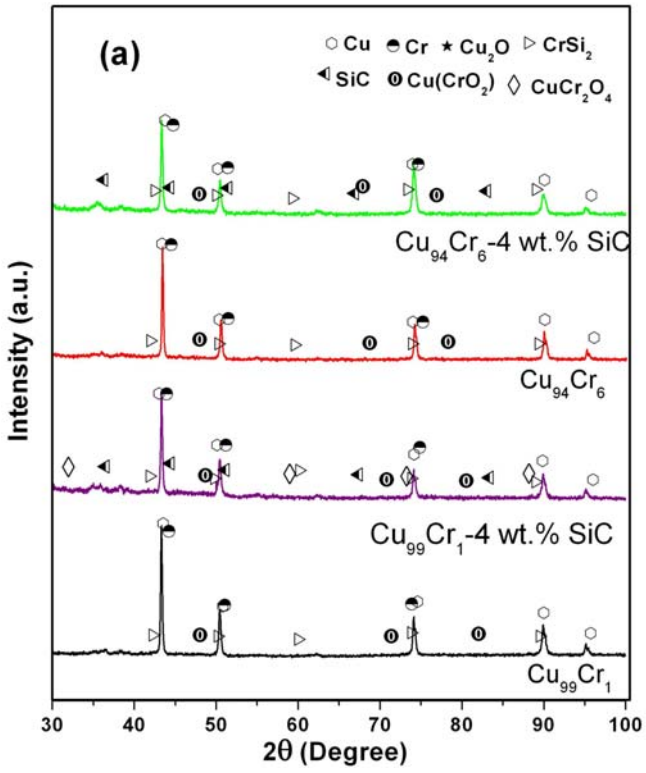

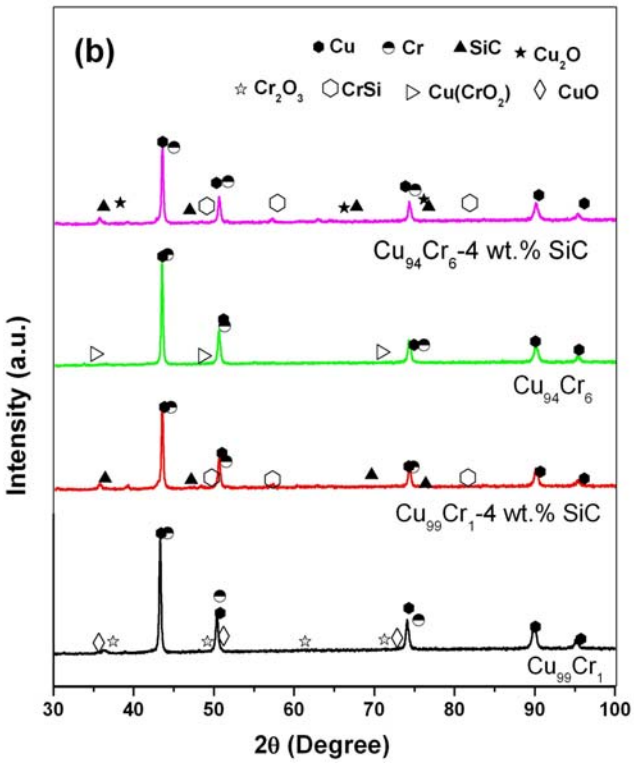

Fig. 4.13: XRD patterns of microwave sintered specimens sintered at (a) 800°C and (b) 900°C.

Peak intensity was found to be sharpened and enhanced with increasing sintering temperature from 900°C to1000°C in case of conventional and vacuum sintering, and 800°C to 900°C in case of microwave sintering as shown figures. Crystallite size of the Cu/Cu-based alloys of the sintered specimens was analyzed from the XRD data and present in Table 4.2. Crystallite size of the conventionally and vacuum sintered specimens at 900°C was measured to be in the range of 101–117 nm, whereas it was in the range of 107–123 nm when sintering temperature was raised to 1000°C. It may be noted that crystallite size of the sintered specimens containing SiC was finer than that of the Cu-Cr compositions at the same sintering temperature. Overall, it can be seen that there is not much variation of crystallite size for conventional and vacuum sintered specimens at a particular sintering temperature.

Microwave sintering was carried out at a much lower temperature (800°C and 900°C) with less soaking period (30 min) compared to other sintering methods in the present investigation. It is observed that there is not much increase in peak intensity of the

XRD patterns of the microwave sintered specimens sintered at 800°C and 900°C than that of 50 h milled sample, whereas, sintered density was found to be maximum compared to that of the other sintering techniques. Crystallite size of the microwave sintered specimens was also found to be much smaller (65–79 nm at 800°C, 68–81 nm at 900°C) than that of the other sintering methods. This is because of the fact that microwaves facilitate energy transfer to the materials, which interacts directly with the particulates within the pressed compact, providing volumetric heating at much faster rates (Clark et al., 1996; Xie et al., 1999; Oghbaei et al., 2010). Moreover, microwave sintering provides relatively homogeneous heating which reduces thermal gradient in the compact compared to conventional heating resulting homogeneous microstructure (Clark et al., 1996; Sutton et al., 1989). Local heating at much higher rate by microwave sintering enhances much faster bonding between the particles which reduces sintering time (Oghbaei et al., 2010). It was also reported that power of microwave field inside the specimens is 30 times higher than the external field, which helps in ionization at the surface of the particles of the compacts. This accelerates the rate of diffusion and hence densification is promoted at much faster rate (Barba et al., 2004; Yadoji et al., 2003; Yan et al., 2006).

Table 4.2: Variation of crystallite size of Cu-based solid solutions for different compositions after sintering by conventional, vacuum, and microwave sintering methods at different temperatures.

Compositions	Average crystallite size of sintered specimen (nm)					
	Conventional sintering		Vacuum sintering		Microwave sintering	
	900°C	1000°C	900°C	1000°C	800°C	900°C
$Cu_{99}Cr_1$	117	123	114	118	79	81
$Cu_{99}Cr_1$–4 wt.% SiC	106	111	104	107	68	72
$Cu_{94}Cr_6$	112	118	109	113	76	79
$Cu_{94}Cr_6$–4 wt.% SiC	101	107	101	106	65	68

AFM analysis

The particle size can be measured from the AFM micrograph of the sintered specimens and VEECO di Innova atomic force microscope was utilized for the study of the average particle size for few sintered samples. Figs. 4.14(a-b) show AFM micrograph for microwave sintered specimens of $Cu_{94}Cr_6$ and $Cu_{94}Cr_6$–4 wt.% SiC, respectively. The average particle size could be estimated to be more than 200 nm for $Cu_{94}Cr_6$ and below 200 nm $Cu_{94}Cr_6$–4 wt.% SiC compositions, respectively. Moreover, micrographs clearly indicate that distribution and morphology of particles is more uniform in case SiC containing composition. Therefore, fine SiC particles not only hinder the coarsening of matrix grains but also control the final distribution of matrix grains.

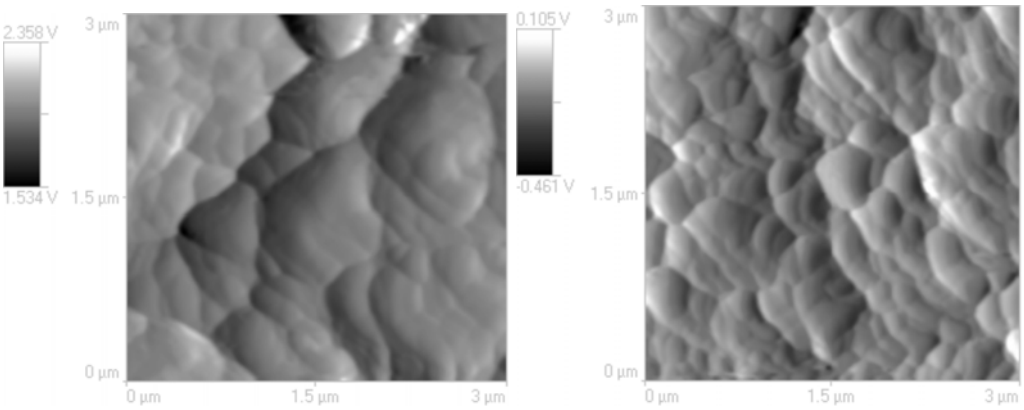

Fig. 4.14: AFM micrographs of microwave sintered specimens of (a) $Cu_{94}Cr_6$ and (b) $Cu_{94}Cr_6$–4 wt.% SiC compositions, respectively.

4.3 Mechanical Properties of Sintered specimens

Mechanical properties, namely, Vickers hardness and wear resistance were evaluated for the sintered specimens. Vickers hardness values were measured for the all sintered specimens and wear resistance was compared for the microwave sintered specimens carried out at 800°C and 900°C.

4.3.1 Vickers hardness

Hardness values of sintered pellets were measured using a Leco LV 700 Vickers hardness tester and it is shown in Table 4.3. Higher hardness values in the range of 189–238 Hv were obtained for the specimens of all compositions sintered at 900°C by microwave sintering method and lowest values in the range of 158–198 Hv were observed in conventionally sintered samples for same compositions. Vickers hardness of the specimens sintered at 1000°C by conventional and vacuum sintering methods was in the range of 170–218 Hv. This indicates that increasing the sintering temperature for these methods increased the sintered density 7–11% compared to the sintered density at 900°C. In case of microwave sintering, sintered density increased only by 1–1.5% when sintering temperature was raised from 800°C to 900°C. This is possibly due the fact that 800°C temperature is sufficient for microwave sintering of the present compositions. This is also supported from the results studied by the dilatation investigation as shown in Fig. 4.9, i.e., compaction by diffusion started at 700°C. It was found that, hardness values were increased by only 2–3% in vacuum sintered specimens compared to that of conventional sintered specimens for all compositions sintered at same temperatures. Whereas, when conventional and microwave sintering were compared hardness values were enhanced by ~20% for microwave sintered specimens. As microwave sintered samples contains very less and small voids and also less grain growth occurred than conventional or vacuum sintered specimens, the hardness values were measured to be higher than that of the other specimens. This is also corroborated with the sintered density of the corresponding specimens (Table 4.1). The hardness of pure Cu is 49 Hv (Goodfellow, 1993/94). Addition of only 1 at.% of Cr in pure Cu increased the hardness about 3.8 times by microwave sintering when the sintered density is ~95% only. It may be also noted that the Vickers hardness value was increased when Cr content increases for a particular sintering method and hardness was found to be further enhanced by adding SiC particles with Cu-Cr compositions.

The hardness values of the conventional and vacuum sintered specimens were increased with increasing sintering temperature from 900°C to 1000°C, possibly due to increased in the sintered density as shown in Table 4.1. The elimination of pores by

coarsening of grains is the main mechanism of sintering by conventional and vacuum sintering techniques, whereas, in microwave sintering densification of compact occurs by different mechanisms. It is known that microwaves interact readily with high dielectric constant material easily (Reddy et al., 2010). The entrapped air in the pores couples with the microwaves, because the entrapped air is having high dielectric constant. Thus this leads to eliminate the pores without much coarsening of the grains. Therefore, it can be concluded that increase in hardness is a function of presence of Cr, hard SiC nanoparticles and sintered density of the specimens. It is also to be noted that enhancement of the sintered density of the SiC containing compositions was much higher when sintering is carried out by microwave sintering. SiC is known to be a good susceptor of microwave. Therefore, during microwave sintering, intense microwave field concentrates around the surface of SiC particles present in the matrix (Saitou et al., 2006). This leads to the local heating at the particle/matrix interface resulted high rate of densification.

Table 4.3: Vickers Hardness (Hv) of different specimens sintered by conventional, vacuum and microwave sintering techniques at different temperatures.

Blend Composition	Hardness of sintered pellets (%), Hv					
	Conventional sintering		Vacuum sintering		Microwave sintering	
	900°C	1000°C	900°C	1000°C	800°C	900°C
$Cu_{99}Cr_1$	158	170	159	173	188	189.8
$Cu_{99}Cr_1$–4 wt.% SiC	190	208	188	212	219	220.5
$Cu_{94}Cr_6$	166	171	167	173	199	200.5
$Cu_{94}Cr_6$–4 wt.% SiC	198	216	197	218	241	238

4.3.2 Wear Resistance

Wear resistance tests were carried out for microwave sintered specimens for all the 4 compositions sintered at two different temperatures, i.e., at 800°C and 900°C. The tests were done using Ball-On-Plate Wear Tester TR-208 M1under a constant load of 5N for 300 S at 15 rpm. Fig. 4.15(a) shows the wear depth vs. time (s) plot for microwave sintered specimens sintered at 800°C. It is clear from this figure that wear resistance of Cu-Cr composition is much lower than that of SiC containing composition. With increase in the Cr content from 1to 6 at.% wear resistance increases as indicated by lower wear depth as shown in Fig. 4.15(a). But with addition of only 4 wt.% of SiC in above mentioned Cu-Cr compositions wear depth decreases to a much lower value (0.55 –2.04 μm) compared to Cu-Cr compositions (2.57–3.02 μm).

As porosity level on the surface of the specimen is high which may be due to improper bonding between particles and oxidation on the surface during sintering, initially it increases the wear depth for all the cases. But with time in the subsurface level as when sufficient lubrication is generated itself due to deformation a constant wear depth was observed. Fig. 4.15(b) shows the wear depth vs. time (s) plot for microwave sintered specimens sintered at higher temperature, i.e., at 900°C. Here also similar trend in wear behavior was observed. But in this case for all compositions wear depth is comparatively little higher than that of the 800°C sintered samples. This could be due to at higher temperature (at 900°C) of sintering there is a chance of grain coarsening/grain growth which actually soften the matrix material. Moreover, wear behavior of these specimens can be corroborated with corresponding values of Vickers hardness (Table 4.3) and relative sintered density (Table 4.1) as discussed earlier.

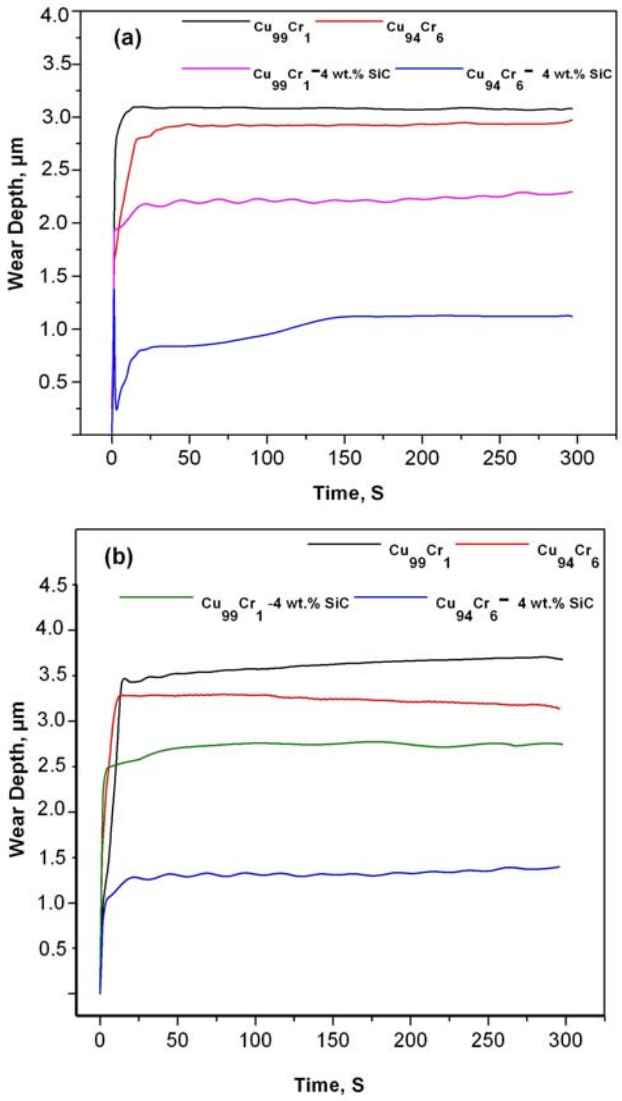

Fig. 4.15: Wear depth vs. time (s) plot for microwave sintered specimens sintered (a) at 800°C and (b) at 900°C.

To corroborate the wear behavior of the microwave sintered specimens, SEM micrographs of the wear track surface were recorded. Figs. 4.16(a-d) show the SEM micrographs of microwave sintered specimens after wear test. It is shown that wear track in case of $Cu_{99}Cr_1$ is clearly visible than other compositions possibly due to higher amount of material was wear out from the surface. When Cr content was increased and harder SiC particles were added the wear resistance was found to be enhanced. This is clearly visible from the SEM micrographs of the corresponding specimen (Fig. 4.16). Fig. 4.16 (d) shows the SEM micrograph of $Cu_{94}Cr_6$–4 wt.% SiC, which clearly indicates that higher amount of applied load was required to carry

out the wear test to make the wear track clearly visible. This basically indicates that wear resistance is much higher than that of the other samples. Therefore, it can be concluded from Figs. 4.15 and 4.16 that wear resistance was found to be increased with increase in Cr content and addition of fine SiC particles.

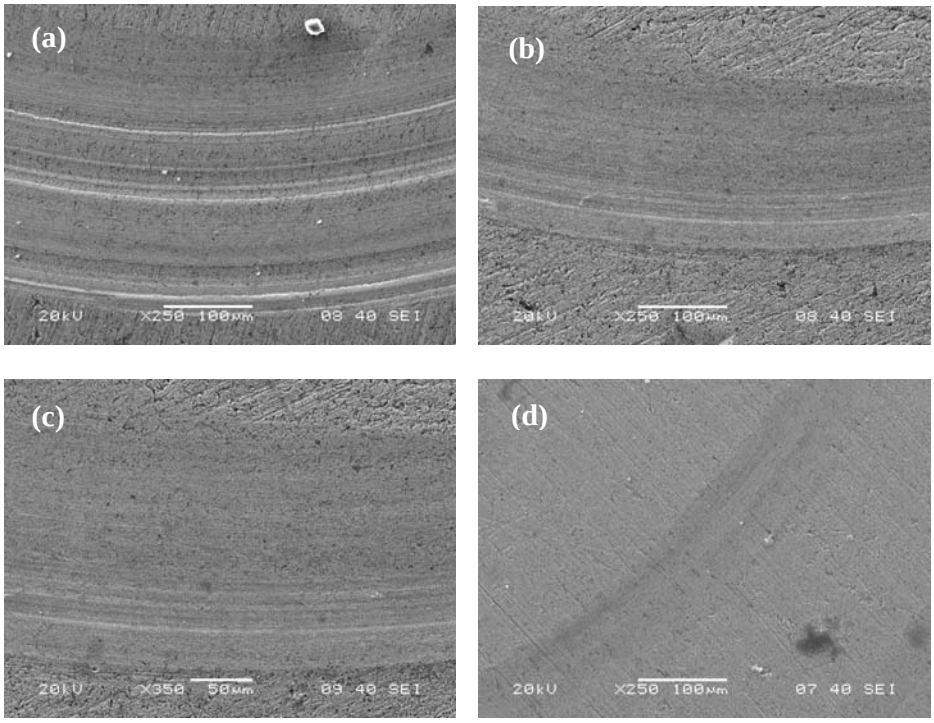

Fig. 4.16: SEM micrographs of microwave sintered specimens of (a) $Cu_{99}Cr_1$, (b) $Cu_{99}Cr_1$–4 wt.% SiC, (c) $Cu_{94}Cr_6$, (d) $Cu_{94}Cr_6$–4 wt.% SiC after wear test.

4.4 Electrical conductivity

Electrical conductivity of the sintered specimens of all the compositions sintered by various methods, namely, microwave sintering, vacuum sintering and conventional sintering were measured and compared with the conductivity as per the International Annealed Copper Standard (IACS) (100%) and listed in the Table 4.4 below. The conductivity was measured using 4-probe method in SIGMATEST D 2.068, FOERSTER instrument.

It can be noted from the Table 4.4 the electrical conductivity gradually increases from the range of 44–54% to 66–68.6% when the sintering method was changed from conventional to microwave sintering techniques. Moreover, when sintering temperature was increased, e.g., 800°C to 900°C in case of microwave sintering, electrical conductivity was found to be higher (65.5–68.6%) than that of the specimens (62–66%) sintered at lower temperature. This is because of the recovery and relaxation of grains, and grain growth, which reduces grain boundary area (Raghavan, 1992). Moreover, at higher temperature a little higher densification was obtained by elimination of porosity. This also helps in improving bonding among particles. These make easier to flow electron and achieve higher conductivity (Rajkovic et al., 2008). But with increasing Cr content from 1 to 6 at.%, it decreased the conductivity slightly and further decreased with the addition of 4 wt.% of nanosize SiC particles with the same composition, although the relative density almost remain in the similar level (Table 4.1). This is expected as because of the electrical conductivity of Cr and SiC is much lower than that of Cu. But, amount of these elements added in present investigation is very low. But after mechanical milling for 50 h, the particle size reduced to a much finer size. Therefore, for a given volume fraction of reinforcement finer size particles would generate more interface area. These interfaces possibly act as source of additional electron scattering. This might be a significant factor in reduction of electrical conductivity. Moreover, matrix (Cu) grain size was found to be finer in case of composition containing higher amount of Cr for the 50 h milled samples. Addition of SiC again refined the matrix grains further for the same duration of milling (50 h) and SiC. It is know that smaller size particles/crystallite size contributes less electrical conductivity. Because grain boundaries acts as a centre of electron scattering (Murty et al., 2007). So the reduction of electrical conductivity in case of $Cu_{99}Cr_1$–4 wt.% SiC is higher than that of $Cu_{94}Cr_6$–4 wt.% SiC compacts for a particular sintering temperature in a particular sintering method.

In present investigation, the highest level of conductivity obtained was in the range of 65–69%, which is much lower if compared with IACS. This could be further increased by improving the sintered density of the materials by employing proper

sintering techniques, like, spark plasma sintering, where, suitable sintering parameters (temperature, pressure, time) can be combined to achieve desired level of densification without much deteriorated the mechanical properties (Angerer et al., 2005).

However, the material developed in the present investigation showed hardness values in the range (200–240) Hv and electrical conductivity of (65–70)% with a densification level of 90–95%. Therefore this material could be successfully used in field of electro-technology, where the devices require high electrical conductivity as well as high strength like electrodes for electrical spot welding, relay blades and contact supports, sliding electrical contacts, and so forth (Lopez et al., 2007).

Table 4.4: Electrical conductivity of different specimens sintered by conventional, vacuum and microwave sintering techniques at different temperatures.

Blend Composition	Electrical Conductivity of sintered pellets (%)					
	Conventional sintering		Vacuum sintering		Microwave sintering	
	900°C	1000°C	900°C	1000°C	800°C	900°C
$Cu_{99}Cr_1$	54	58	53.4	60	66	68.6
$Cu_{99}Cr_1$–4 wt.% SiC	46.4	54.8	46.2	54	63	66
$Cu_{94}Cr_6$	53	55.8	53.3	58	65	67
$Cu_{94}Cr_6$–4 wt.% SiC	44	53.4	45.5	53	62	65.5

CHAPTER 5 Conclusions and Future Scope of Study

5.1 Conclusions

a) In the present investigation attempts have been made to synthesize bulk Cu-based nanocomposites of $Cu_{99}Cr_1$, $Cu_{94}Cr_6$, $Cu_{99}Cr_1$–4 wt.% SiC and $Cu_{94}Cr_6$–4 wt.% SiC compositions reinforcing with a small amount of Cr and/or SiC particles developed by mechanical milling (milled for 50 h) followed by microwave sintering (800°C and 900°C, 30 min), vacuum sintering (900°C and 1000°C, 60 min) and conventional pressure-less sintering (900°C and 1000°C, 60 min) methods.

b) Formation of Cu-Cr solid solution by mechanical milling detected to be very small (< 1 at.%). This could be noticed from the XRD data and variation of lattice parameters of Cu-based solid solution with the progress of milling. The solubility of Cr in Cu also is very small as per the equilibrium phase formation of Cu-Cr alloys (<0.03 at.% at 400°C).

c) Dilatation measurement indicated that sintering of the mechanically milled specimens above 700°C could generate bulk consolidated specimens.

d) XRD and AFM analysis of the sintered samples revealed that the crystallite size was in the range of 65–125 nm and average particle size was < 200 nm in size, respectively. Crystallite/particles size was found to be much finer in SiC reinforced composites.

e) Enhancement in the relative sintered density (with respect to theoretical density) was observed by microwave sintering method (90.8–95%) compared to vacuum sintering (84.2–89%) and conventional pressure-less sintering (82.3–87%) methods.

f) Vickers hardness of microwave sintered compacts were found to be in the range of 190–240 Hv depending on variation of composition, compared to 173–218 Hv for vacuum sintered and 170–216 Hv for conventionally sintered specimens of same compositions.

g) Wear resistance of the microwave sintered specimens was found be increased with in Cr content and also addition of nanosize SiC particles.

h) The microwave sintered compacts showed greatly superior mechanical properties compared to the vacuum sintered and pressure-less sintered compacts, possibly due to the presence of much finer microstructural features and better densification.

i) Electrical conductivity of the microwave sintered specimens showed 60–70% conductivity of IACS compared to 40–50% for conventional and vacuum sintered compacts.

j) Therefore, microwave sintering is found to be most effective in consolidation of Cu-Cr or Cu-Cr–SiC nanocomposite powders compared to the other methods used in the present investigation as suitable combination of mechanical and electrical properties were obtained using this technique. Therefore the material developed in the present investigation could be successfully used for thermo-electric applications.

5.2 Future Scope of Study

a) Cu-based nanocomposites could be developed with higher amount of reinforcements (Cr and/or SiC etc.) in more intensive grinding media to enhance mechanical properties further.

b) Consolidation could be carried out using some advance techniques like high pressure torsion (HPT) or spark plasma sintering (SPS) method to achieve nearest to theoretical density (>95%) retaining nano-features in the bulk specimens, as increase in the density would improve mechanical as well as electrical conductivity.

c) Details study of the wear behavior is to be carried out for all the sintered specimens.

References

Akhtar F, Askari SJ, Shah KA, Duac X, Guo S. Mater Charac 60 (2009) p. 327.

Anderson KR, Groza JR. Metall Mater Trans A 32 (2001) p. 1211.

Angerer P, Yu LG, Khor KA, Korb G, Zalite I. J Eur Cer Soci 25 (2005) p. 1919.

Anklekar RM, Agrawal DK, Roy R. Powd Metall 44 (2001) p. 355.

Anklekar RM, Bauer K, Agrawal DK, Roy R. Powd Metall 48 (2005) p. 39.

Barba A, Clausell C, Feliu C, Monzo M. J Amer Cer Soci 87 (4) (2004) p. 571.

Benjamin J. Metall Trans A 1 (1970) 2943.

Brandes EA, Brook GB (Eds.). Smithells Metals Reference Book, 7th ed., (1992), p.42.

Broyles SE, Anderson KR, Groza JR, Gibeling JC. Metal Mater Trans A 27 (1996) p. 1217.

Chang SY, Lin SJ. Script Mater 35 (1996) p. 225.

Clark DE, Binner JGP, Lewis DA, editors. Ceram Trans. Westerville (OH): The American Ceramic Society 111 (2001).

Clark DE, Sutton WH. Annual Rev Mater Sci 26 (1996) p. 299.

Correia JB, Davies HA, Sellars CM. Acta Mater 45 (1997) p. 177.

Das D, Samanta A, Chattopadhyay PP. Mater Manuf Proces 22 (2007) p. 516.

Das S, Mukhopadhyay AK, Datta S, Basu D. Bull Mater Sci 32 (2009) p. 1.

Dehm G, Thomas J, Mayer J, Weissgarber T, Pusche W, Sauer C. Philos Mag A 77 (1998) p. 153.

Deshpande PK, Lin RY. Mater Sci Eng A 418 (2006) p. 137.

Dong SJ, Zhou Y, Shi YW, Chang BH. Metall Mater Trans A 33 (2002) p. 1275.

Dong SR, Tu JP, Zhang XB. Mater Sci Eng A 313 (2001) p. 83.

Eckert J. Nanostructured materials-processing, properties and potential applications. Noyes Publications, New York, (2002) p 423.

Ellis TW, Kim ST, Verhoeven JD. JMEPEG 4 (1995) p. 581.

Fan GJ, Choo H, Liaw PK, Lavernia EJ. Mater Sci Eng A 409 (2005) p. 243.

Froes FH, Suryanaryana C. JOM 41 (1989) p. 16.

Gautam RK, Ray S, Jain SC, Sharma SC. Wear 265 (2008) p. 902.

Gedevanishvili S, Agrawal D, Roy R. J Mater Sci Lett 18(1999) p. 665.

Gleiter H. Nanostruct Mater 1 (1992) p. 1.

Goodfellow. Metals, Alloys, Compounds, Ceramics, Polymers, Composites. Catalogue 1993/94.

Groza JR. Nanocry Powder Consolidation Methods, in, Nanostructured Materials-Processing, Properties and Potential Applications, edited by C.C. Koch, Noyes, New York, (2002) p. 115.

Guduru RK, Murty KL, Youssef KM, Scattergood RO, Koch CC. Mater Sci Eng 463 (2007) p.14.

Guler O, Evin E. j Mater Proces Tech 209 (2009) p. 1286.

Hahn H, Mondal P, Padmanabhan KA. Nanostruct Mater 10 (1997) p. 603.

Hashemi HN, Aziri A, Ziemer K. Mater Sci Eng A 478 (2008) p. 390.

Huber E, Frohlich K, Grill R. Trans Plasma Sci 25(4) (1997) p. 642.

Iskander MF, Kiggans Jr JO, Bolomey JC, editors. Mater Res Soc Symp Proc, Warrendale (PA): Materials Research Society, 430 (1996).

Jena PK, Brocchi EA, Solorzano IG, Motta MS. Mater Sci Eng A. 371 (2004) p. 72.

Jovanovic MT, Rajkovic V. MJoM 15 (2) (2009) p. 125.

Kear BH, McCandish LE, Nanostruct Mater 3 (1993) p. 19.

Koch CC. J Met Nano Mater 18 (2003) p. 9.

Koch CC. Nanostruct Mater 9 (1997) p. 13.

Kwon DH, Nguyen TD, Huynh KX, Choi PP, Chang MG, Yum YJ, Kim JS, Kwon YS. J Cer Proce Res 7(3) (2006) p. 275.

Lahiri I, Bhargava S. Mater Char 60 (2009) p. 1406.

Lahiri I, Bhargava S. Powd Tech A 189 (2009) p. 433.

Lee KL, Whitehouse AF, Hong SI, Russell AM. Metal Mater Trans 35 (2004) p. 695.

Lee YF, Lee SL, Huang CH, Lee CK. Powd Metall 44 (2001) p. 339.

Liang S, Fan Z, Xu L, Fang L. Composites Part A: Appl Sci Manuf 35 (2004) p. 1441.

Liu JL, Wang ED, Liu ZY, Hu LX, Fang WB. Mater Sci Eng A 382 (2004) p. 301.

Lopez M, Jimenez JA, Corredor D. Composites A 38 (2007) p. 272.

Ma ZY, Tjong SC. Mater Sci Eng A 284 (2000) p. 70.

Marques MT, Ferraria AM, Correia JB, Botelho do Rego AM, Vilar R. Mater Chem Phys 109 (2008) p. 174.

Marques MT, Livramento V, Correia JB, Almeida A, Vilar R. J. Alloys Compd. 48 (2007) p.434.

Morris DG. Trans Tech Publ (1998) p. 1.

Morris MA, Morris DG. Acta Metal 35 (1987) p. 2511.

Morris MA, Morris DG. Mater Sci Eng 104 (1988) p. 201.

Mula S, Ghosh S, Pabi SK. Mater Sci Eng, 472 (2008) p. 208.

Murphy R, Grant NY, Powder Met 5 (1992) p. 1.

Murty BS, Venugopal T, Rao KP. Acta Metall 55 (2007) p. 4439.

Oghbaei M, Mirzaee O. J Alloy Comp 494 (2010) p. 175.

Peng LM , Ma XM, Xu KD, Ding WJ. Mater Proc Tech 166 (2005) p. 193.

Raghavan V. Physical metallurgy Principles and Practice, Prentice Hall of India, (1992).

Rajkovic V, Bozic D, Jovanovic MT, J. Alloy comp 459 (2008) p. 177.

Rajkovic V, Bozic D, Jovanovic MT. J Mater Proces Tech 200 (2008) p. 106.

Reddy GC, Rajkumar K, Aravindan S. Int J Adv Manuf Tech 48 (2010) p. 645.

Roy R, Agrawal D, Cheng J, Gedevanishvili S. Nature 399 (1999) p. 668.

Saitou K. Scrip Mater 54 (2006) p. 875.

Sauvage X, Jessner P, Vurpillota F, Pippan R. Script Mater 58 (2008) p. 1125.

Scattergood RO, Koch CC, Murty KL, Brenner D. Mater Sci Eng 493 (2008) p.3.

Shehata F, Fathy A, Abdelhameed M, Moustafa SF. Mater design 30 (2009) p. 2756.

Shen YF, Lu L, Lu QH, Jin ZH, Lu K. Scrip Mater 52 (2005) p. 989.

Shull RD, Ritter JJ, Shapiro AJ, Swartzendruber LY, Bennet LH. J Appl Phy 63 (1990) p.4261.

Suryanarayana C. Prog Mater Sci 46 (2001) p.184

Sutton WH, Amer Cer Soci Bull 68 (2) (1989) p. 376.

Tjong SC, Lau KC. Mater Lett 43 (2000) p. 274.

Tjong SC, Lau KC. Mater Sci Eng A 282 (2000) p. 183.

Upadhyaya A, Upadhyaya GS. Mater Design 16 (1995) p. 41.

Wan YZ, Wang YL, Cheng GX, Tao HM, Cao Y. Powd Metal 41 (1998) p. 59.

Weertman JR. Mech Behav Nanocry Met, in, Nanostructured Materials-Processing, Properties and Potential Applications, edited by C.C. Koch, Noyes, New York, (2002) p. 397.

Xie Z, Yang J, Huang X, Huang Y. J Eur Cer Soci 19 (1999) p. 381.

Yadoji P, Peelamedu R, Agrawal D, Roy R. Mater Sci Eng B 98 (2003) p. 269.

Yan M, Hu J, J Magn Mag Mater 305 (2006) p. 171.

Zhu J, Liu L, Zhao H, Shen B, Hu W. Mater Design 28 (2007) p. 1958.

Zuhailawati H, Mahani Y. J. Alloys Comp 476(2009) p. 142.

List of Publications

- **P. Sahani** and Suhrit Mula. "Synthesis and characterization of copper-chromium–SiC nanocomposites by high energy ball milling." Selected for **3rd best paper award at International conference ICON 2010, on 5-6 march 2010, Coimbatore.**
- **P. Sahani,** S. K. Pratihar and Suhrit Mula. Mechanical and electrical properties of copper-based nanocomposites developed by microwave sintering for thermo-electric applications. Manuscript being prepared. To be communicated shortly.